

Eastern Michigan University
DigitalCommons@EMU

Master's Theses and Doctoral Dissertations

Master's Theses, and Doctoral Dissertations, and
Graduate Capstone Projects

7-14-2016

Synthesis and structure activity relationship of novel small molecules as inhibitors of plasminogen activator inhibitor-1

Karl Michael Upman

Follow this and additional works at: <http://commons.emich.edu/theses>

 Part of the [Chemistry Commons](#)

Recommended Citation

Upman, Karl Michael, "Synthesis and structure activity relationship of novel small molecules as inhibitors of plasminogen activator inhibitor-1" (2016). *Master's Theses and Doctoral Dissertations*. 679.
<http://commons.emich.edu/theses/679>

This Open Access Thesis is brought to you for free and open access by the Master's Theses, and Doctoral Dissertations, and Graduate Capstone Projects at DigitalCommons@EMU. It has been accepted for inclusion in Master's Theses and Doctoral Dissertations by an authorized administrator of DigitalCommons@EMU. For more information, please contact lib-ir@emich.edu.

Synthesis and Structure Activity Relationship of Novel Small Molecules as Inhibitors of
Plasminogen Activator Inhibitor-1

by

Karl Michael Upman

Thesis

Submitted to the Department of Chemistry

Eastern Michigan University

in partial fulfillment of the requirements

for the degree of

MASTER OF SCIENCE

in

Chemistry

Thesis Committee:

Cory Emal, PhD, Chair

Gregg Wilmes, PhD

Maria Milletti, PhD

Ypsilanti, Michigan

July 14, 2016

DEDICATION

I would like to dedicate this thesis to my parents, Mike and Paula, who have supported my entire career as a student. They ensured I attended an excellent undergraduate college despite the distance, cost, and challenge. They further supported me post-graduation and vaulted me towards my master's degree. Both of my parents are strong role models and are impeccable at lending guidance.

I would also like to dedicate this to my friends who have aided me more than they may realize. Their ability to alleviate stress and promote priorities over all else when I faltered is something I could never have gone without.

Finally, I would like to dedicate this thesis to my wife, Erica. Without her my entire master's degree would not have been feasible. She supported me both mentally and financially, every day for the duration of my degree and this project. To her, I owe my success.

ACKNOWLEDGMENTS

First and foremost, I would like to extend my deepest gratitude to my research advisor, Dr. Cory Emal. He has perfected the balance of motivating students and allowing them to handle their own responsibilities, and without his guidance and teaching, I would not have had the pleasant experience I experienced during graduate school. He was capable of being not only an exceptional mentor but a friend as well.

I would also like to thank Dr. Gregg Wilmes for lending his knowledge reliably throughout my research and Christina Varney who through insight and example helped motivate me from the moment I entered Eastern.

Although we have never met personally, I would like to send my gratitude to Dr. Daniel Lawrence of University of Michigan and his research group for providing quick and precise assay results. I would also like to acknowledge the role that every professor I had at Eastern Michigan University had in my success. Every class I attended was truly one of the best learning experiences of my career and each professor ensured that I, along with all of the other students, flourished. The graduate program at Eastern Michigan University provided me with all of the necessary tools I needed to be successful, and for that I am deeply appreciative.

Abstract

Plasminogen activator inhibitor type-1 (PAI-1) is a member of the serine protease inhibitor (serpin) family. PAI-1 is involved in the regulation of fibrinolysis, which is the breakdown of blood clots. PAI-1 inhibits serine proteases tissue-type plasminogen activator (tPA) and urokinase-type plasminogen activator (uPA), which are key factors in fibrinolysis. Excess levels of PAI-1 have also been shown to increase the risk of diabetes, stroke, and atherosclerosis, as well as tumor development. Previous attempts at synthesizing a practical drug for the regulation of PAI-1 have not been successful; therefore, it has been the purpose of this study to further advance progress in this area. Working from a lead molecule derived from a high-throughput library screen, different derivatives were synthesized and tested for anti-PAI-1 activity. By studying the relationships between different aromatic substitutions, our goal was to discover a connection between these substitutions and more potent inhibition of PAI-1. This study discusses the synthesis and impact of the different derivatives of those small molecules on PAI-1 inhibition.

TABLE OF CONTENTS

DEDICATION.....	i
ACKNOWLEDGMENTS.....	ii
ABSTRACT.....	iii
LIST OF TABLES & SCHEMES.....	v
LIST OF FIGURES.....	vi
CHAPTER I.....	1
I-1: Plasminogen Activator Inhibitor-1: Interactions and Diseases.....	1
I-2: PAI-1 Structure.....	3
I-3: Previous PAI-1 Inhibitors.....	6
REFERENCES.....	18
CHAPTER II.....	21
II-1: Novel Small Molecule Inhibitors.....	21
II-2: Aromatic Substituent Variations.....	21
II-3: Extension of Core Chain Length Analogues.....	25
II-4: Alpha-Beta Unsaturated Malonyl Derivatives.....	30
II-5: Conclusions.....	38
EXPERIMENTAL METHODS & DATA.....	40

List of Tables

<u>Table</u>	<u>Page</u>
1. Sulfonamide and sulfonimide based inhibitors.....	15
2. Oxalyl core benzene ring substituent variations.....	23
3. Malonyl-based compounds.....	28
4. Succinyl-based compounds.....	28
5. Previously synthesized inhibitors.....	29
6. Direct comparison of varying core length inhibitors.....	30

List of Schemes

<u>Scheme</u>	<u>Page</u>
1. Synthesis of lead molecule analogs from benzene ring substitutions.....	22
2. Syntheses of malonyl & succinyl compounds with varying end moieties.....	27
3. Synthesis of alpha-beta unsaturated malonyl derivatives.....	31
4. Synthesis of alpha-beta unsaturated malonyl derivative using butyraldehyde.....	31
5. Synthesis of alpha-beta unsaturated malonyl derivative using nonanal.....	32
6. Synthesis of alpha-beta unsaturated malonyl derivative using veratraldehyde.....	33
7. Formation of hydrazide from alpha-beta unsaturated malonyl compound.....	35
8. Alternate synthesis for the formation of hydrazide malonyl compound using veratraldehyde.....	36
9. Alternate synthesis for the formation of hydrazide malonyl compound using butyraldehyde.....	36
10. Synthesis of hydrazone with veratraldehyde.....	38

List of Figures

<u>Figure</u>	<u>Page</u>
1. Structure of Plasminogen Activator Inhibitor-1.....	3
2. Pathway and forms of PAI-1.....	4
3. PAI-1 interactions with vitronectin.....	5
4. Second generation synthesized compounds.....	13
5. Locations of analogue syntheses.....	21
6. Malonyl & Succinyl cores.....	26
7. NOESY data of CDE-512.....	34
8. Hydrazone butyraldehyde product reaction.....	37
9. Hydrazone product of veratraldehyde.....	37

Chapter I

I-1: Plasminogen Activator Inhibitor-1: Interactions and Diseases

Plasminogen activator inhibitor-1 (PAI-1) is a protein present in all mammals, including humans. PAI-1 is present in low amounts in the body, but even in such small concentrations, it has a large impact on human health. PAI-1 has various roles in the body, but the primary one is to regulate fibrinolysis. Fibrinolysis occurs via the conversion of plasminogen, an inactive protein, into the enzyme plasmin, which then degrades fibrin clots into products able to be used by the body in other functions. When PAI-1 binds with tissue-type plasminogen activator (tPA) and urokinase-type plasminogen activator (uPA), it inhibits the conversion of plasminogen (a zymogen) into active plasmin, thus regulating the cycle. Therefore, it is understood that an excess of PAI-1 can lead to hypofibrinolysis: an increase in the level of blood clots.¹⁻³ This has led to a number of studies that have connected PAI-1 to various blood related diseases such as thromboembolism, coronary artery disease, sepsis, myocardial infarction, as well as cancer, atherosclerosis, and type 2 diabetes.¹⁻³

This is immediately concerning because it shows that PAI-1 is capable of holding multiple different pathological roles, based on its connection to each disease. When an excess of PAI-1 is present and hypofibrinolysis occurs, it is thought that there is a parallel increase in the pathogenesis of atherosclerosis by exposing arteries to chronic thrombosis.³ With the acceleration of angiogenesis brought on by PAI-1, cancer is able to progress.⁴⁻¹⁰ PAI-1 has also been seen to have a relationship with increased levels of amyloid beta in the brain. Amyloid beta has been known to increase amyloid plaques, thought to cause Alzheimer's disease.¹¹ Studies have shown that removing the PAI-1 gene can lead to increased levels of plasmin and tPA, and decreased levels of amyloid beta in the brain.¹²

As previously stated, PAI-1 has been linked to various blood diseases; specifically, in high concentrations PAI-1 was found to be linked to coronary artery disease as well as atherosclerosis and myocardial infarction. With PAI-1 in abundance, the balance of fibrin to fibrin degradation products is severely skewed. This causes plaque buildup and poor regulation in the arteries of the heart, which in turn can cause hardening of these blood vessels and leads to more disastrous results, such as heart failure.^{13,14}

In a study where mice were engineered to produce no PAI-1, many of these diseases were studied. It was found that prognosis of atherosclerosis, thrombosis, and diabetes-induced nephrosis was noticeably improved. This not only showed that PAI-1 is a factor in these diseases, but also that reducing PAI-1's levels may aid in preventing them significantly.¹⁵⁻¹⁹ A similar study conducted with PAI-1 deficiency was shown to prevent obesity as well as a development of resistance to insulin.³ Other studies have suggested that a deficiency of PAI-1 can aid in the prevention of excess fibrin accumulation and bleomycin-induced fibrosis in the lungs.²⁰ In contrast, abnormally low levels of PAI-1 also have their drawbacks. PAI-1 deficiency has been found to be associated with spontaneously developed age-dependent cardiac-selective fibrosis.²¹

There exist a few therapies that can aid in some of these diseases; however, many of these therapies (ACE inhibitors, insulin-sensitizing agents, and hormone replacements) have been found to indirectly boost fibrinolysis, making them not viable for long term use.²² Therefore, it has been deemed extremely beneficial, considering PAI-1's vast pathologically active network, to find regulatory agents specific for PAI-1. Considering it has been a high value drug target, many attempts have been made to find inhibitors of PAI-1.

I-2: PAI-1 Structure

PAI-1 is a member of the serine protease inhibitor superfamily. While also known as endothelial PAI-1 or serpin E₁, it is encoded by the *serpine1* gene.²³ It is primarily synthesized by tissues of the liver, vascular and adipose; however, it is also stored and secreted by varying methods.^{24,25} In humans, PAI-1 is located at chromosome 7q21.30q22, spans about 12,200 base pairs and is composed of nine exons and eight introns.^{26,27} It is a single chain glycoprotein composed of 379 amino acid residues while its secondary structure is composed of 3 β -sheets, 8 or 9 α -helices and a very important reactive center loop (RCL).^{28,29} A structure of PAI-1 is shown in **Figure 1**, but it is also important to know there are other forms of PAI that contribute to its mechanisms and activity. Most notably, PAI-1 has forms known as active, the Michaelis complex, covalent and cleaved.



Figure 1. Structure of plasminogen activator inhibitor-1³⁰

Shown in **Figure 1** is the active form of PAI-1. During this stage the RCL (seen above in red) is exposed and available for bonding to tissue-type and urokinase-type plasminogen activators (tPA & uPA). When this occurs, PAI-1 enters a non-covalent Michaelis complex

(Figure 2).^{31,32} This acts as an intermediate stage where one of two different pathways may occur, leading to either the cleaved or latent forms of PAI-1. The RCL undergoes proteolysis and its amino-terminal end will begin to flip 180 degrees and insert into a second location near the bottom of the molecule. During this time, if the protease, either tPA or uPA, is able to complete its catalytic cycle before insertion of the RCL, PAI-1 will take on its inactive cleaved form, while regenerating the active form of the protease. However, if the protease is not capable of completing its cycle, it will become trapped in the cleaved form of PAI-1 and become inactive.³²

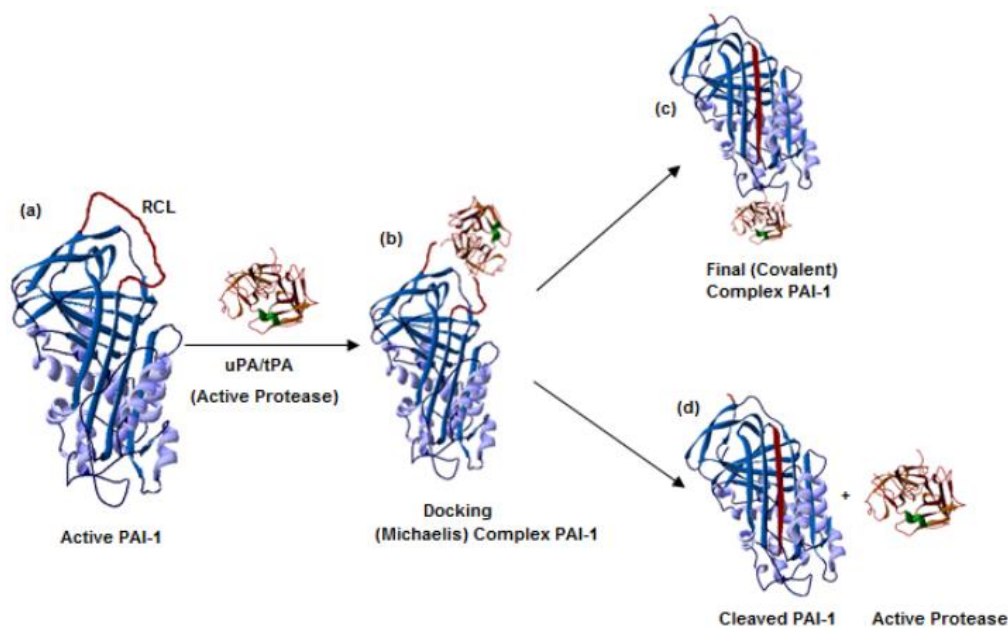


Figure 2. Pathway and forms of PAI-1³⁰

While these are the typical pathways there also exist some instances that further complicate PAI-1's mode of action. It is possible that PAI-1 will spontaneously convert from its active form into its latent form at a half-life of approximately 1 to 2 hours. This prevents any interactions with active proteases and is reported to occur via conformational changes that allow certain strands of the molecule to slide in and out of place to allow the RCL insertion into a β -

sheet.^{28,33-39} It is also possible for PAI-1 to be affected by its environment. In the presence of vitronectin, a glycoprotein found in the extracellular matrix of humans that promotes cell adhesion and motility, PAI-1 can undergo a conformational change that affects the conformation of the RCL.⁴⁰ As seen in **Figure 3**, PAI-1 can bind with vitronectin specifically via the N-terminal somatomedin-B domain on vitronectin; this stabilizes PAI-1 in its active form, rendering the RCL unavailable to uPA.^{34,41}

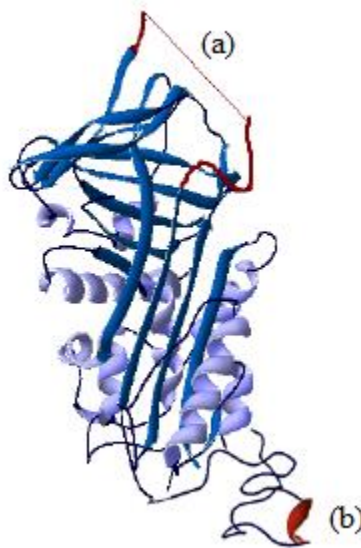


Figure 3. PAI-1 interactions with vitronectin. (a) RCL (b) Vitronectin binding location.³⁰

The interactions of PAI-1 with vitronectin have been found to be able to exceed a 1:1 stoichiometric ratio, which correlates with increased binding of the PAI-1: vitronectin complex to cells.⁴² The PAI-1: vitronectin complex is found to be twice as stable as free PAI-1, lengthening PAI-1's half-life to upwards of 24 hours.³⁹ However, the primary concern with vitronectin is that when it binds with PAI-1, it causes a conformational change to the binding site on PAI-1. While PAI-1 is bound to vitronectin, oligomers of vitronectin begin to form. During this stage tPA can bind to PAI-1, although this process is strained, and force vitronectin to dissociate from PAI-1.

When this occurs it is possible for the oligomers of vitronectin to cleave into monomers, further negatively affecting the cycle involving PAI-1 and its proteases.⁴²

I-3: Previous PAI-1 Inhibitors

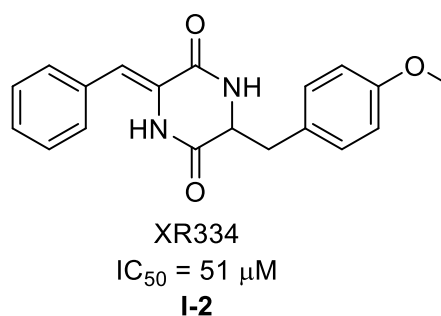
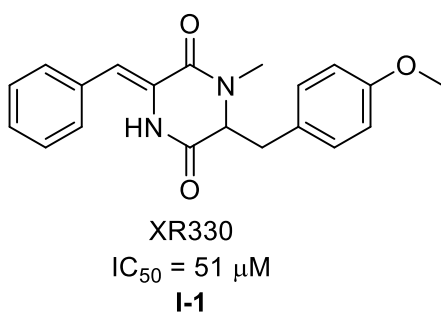
Since the discovery of PAI-1 there have been many attempts to develop inhibitors for it. Monoclonal antibodies (MA) were found to be one of the first direct inhibitors of PAI-1 activity. Initial MAs were found to act upon PAI-1 in several ways: impeding formation of the Michaelis complex that PAI-1 forms when binding with tPA/uPA, inducing behavior that cleaves PAI-1 thereby rendering it inactive, and promoting conversion to the latent form of PAI-1 at an increased rate.^{33,37,43-46} While these MAs appeared to be strong candidates for the inhibition of PAI-1, they proved to fall short in bioavailability as they were quickly degraded via enzymes when taken orally, therefore requiring intravenous injections.

Related studies also looked into the effect of peptides on PAI-1 activity as it was found that certain sequences could inhibit PAI-1 function. The peptides were able to modify the conformation of active PAI-1 by acting upon its reactive site loop. For example, a 14 chain amino acid peptide P14-P1 was shown to hasten the conversion of PAI-1 to its latent form.⁴⁷ Another peptide was remarkably found to inhibit the binding of PAI-1 to vitronectin, which would also accelerate conversion to the latent form, largely reducing activity.⁴⁸ To much disappointment, however, it was concluded that peptides proved too unstable to be administered orally, similarly to the monoclonal antibodies. In addition, they exhibited great difficulty in crossing the blood-brain barrier, making them problematic in treating neurological disorders.

The need for a more specific and bioavailable approach lead to the development of small molecule inhibitors of PAI-1. There were a few attempts using previously discovered drugs or

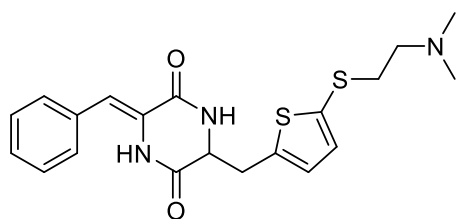
molecules to combat PAI-1. Molecules that were discovered to possess some inhibitory effects were fibrates, herbal medicines, and butadiene derivatives. One of these fibrates, gemfibrozil, developed by Fujii et al. was originally shown to help lower lipid levels.⁴⁹ It also was shown to aid in decreasing levels of PAI-1 in human hepatoma cells.⁴⁹ However, other fibrates were actually found to increase PAI-1 levels in humans, and further, some fibrates were shown to hold no effect on PAI-1.⁴⁹ Studies were then performed comparing different fibrates, and it was found that overall effectiveness greatly depended on type and concentration; however, after further studies, it was hypothesized that PAI-1 secretion could vary among different types of cells making it difficult to control, therefore requiring a better understanding of PAI-1 in order to develop new drugs for it specifically.⁴⁹

It was then concluded that designing small orally effective molecules designed with PAI-1 inhibition in mind would be the most reasonable pathway. The first small molecule inhibitors of PAI-1, synthesized by Xenova Limited, were diketopiperazines (DKP) derivatives XR330 (I-1) and XR334 (I-2). Isolated from a species of *Streptomyces*, these were capable of inhibiting PAI-1's interaction with tPA *in vitro* with an IC₅₀ of 51 μM.

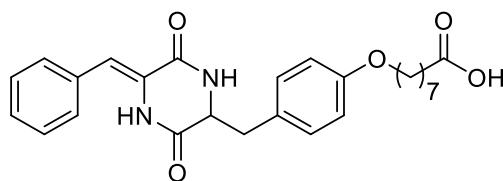


These molecules had limited solubility and were found to enhance fibrinolysis.⁵⁰ Subsequent analogs XR1853, XR5082, XR5118, and XR11211 were developed which also inhibited PAI-1 activity with IC₅₀ values from 3.5-80 μM. These derivatives worked by encouraging the formation of the latent form of PAI-1, or by inhibiting the binding of PAI-1 to tPA/uPA via

structural changes to PAI-1. Of these compounds, XR5118 (I-3) was selected for further studies *in vivo*. XR5118 showed increased inhibition of PAI-1 and was the most selective and even enhanced fibrinolysis while it increased tPA activity in the plasma, indicating a possible treatment for thrombotic disease.⁵¹ XR11211 (I-4) was also studied further as it was also shown to be effective against PAI-1 with an IC_{50} of 0.20 μ M. However, it suffered from poor physiochemical properties, and though there were attempts to improve it, development costs and likelihood of success seemed not worth the effort. These diketopiperazines all seemed to suffer the same fate as XR11211, as they had poor physiochemical properties and were therefore set aside for a new attempt at counteracting PAI-1.⁵¹⁻⁵³



XR5118
 $IC_{50} = 3.5 \mu$ M
I-3

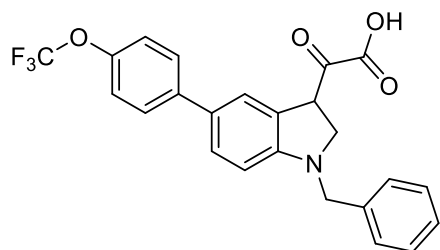


XR11211
 $IC_{50} = 0.20 \mu$ M
I-4

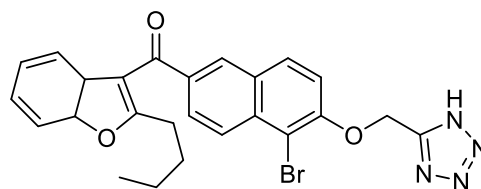
One of the most analyzed small molecule inhibitors has been tiplaxtinin (I-5). With an *in vitro* IC_{50} value of 2.7 μ M, experimentally shown to contain *in vivo* selective activity against PAI-1 in rats, as well as admirable bioselectivity and low toxicity, it appeared to be the front runner in small molecule inhibitors.⁵⁴ Despite all of this, however, it was found that tiplaxtinin in the presence of vitronectin lost nearly all of its ability to inhibit PAI-1. This suggests that the binding site for both tiplaxtinin and vitronectin overlap.^{55,56} This prompted further research into how tiplaxtinin's mechanism of action proceeds. Utilizing surface plasmon resonance (SPR) analysis it was discovered that tiplaxtinin will only bind to free PAI-1 and that once PAI-1 is bound to either vitronectin or becomes latent, there was no observed binding of tiplaxtinin to

PAI-1.⁵⁶ When it is able to bind, it does so reversibly and with an IC_{50} of 9 to 12 μM . During this binding there is anti-proteolytic activity against uPA and tPA.

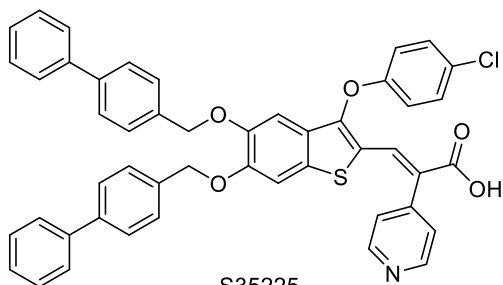
Wyeth researchers reported a number of PAI-1 inhibitors as well, of which the leading molecule was WAY-140312 (I-6). WAY-140312 was found to inhibit PAI-1 with an IC_{50} value of 11.7 μM , yet it also reduced thrombosis after oral administration in an *in vivo* vascular injury study. However, its bioavailability was only 29% and its half-life was extremely short.⁵⁷ A later *in vitro* study in rat and human plasma found that WAY-140312 lost its activity against PAI-1 due to the presence of vitronectin, much like tiplaxtinin did.^{55,58} In another study WAY-140312 and tiplaxtinin were tested side by side against a molecule developed by Rupin and co-workers, S35225 (I-7), a benzothiophene derivative.⁵⁸ In the presence of vitronectin in rat *in vitro* and *in vivo* models, it was discovered that only S35225 had activity against PAI-1. While it was effective intravenously in a dose dependent manner, its half-life was not beneficial for long term use, as it could not be orally administered.⁵⁸



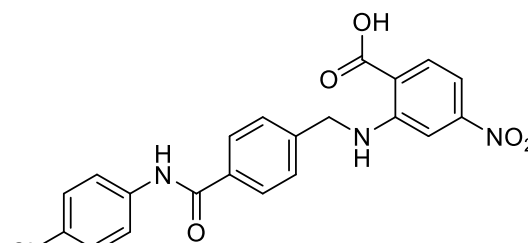
Tiplaxtinin
 $IC_{50} = 2.7 \mu M$ (9-12 μM)
I-5



WAY-140312
 $IC_{50} = 11.7 \mu M$
I-6



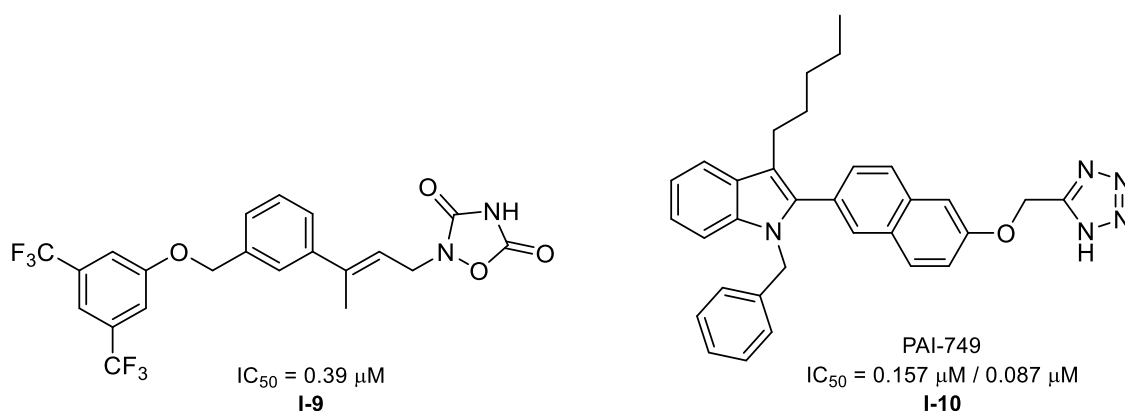
S35225
I-7



AR-H029953XX
 $IC_{50} = 12 \mu M$
I-8

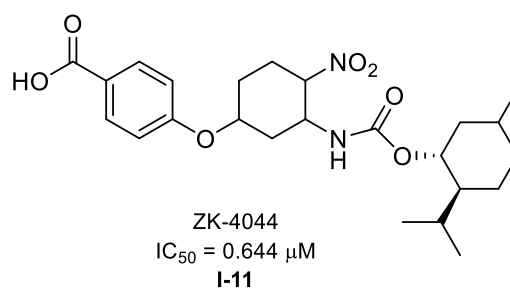
A study performed by Bjorquist et al. attempted to look at flufenamic acid derivatives and found that AR-H029953XX (I-8) inhibits PAI-1 with an IC_{50} of 12 μM .⁵⁹ After a structure-activity relationship analysis, it was concluded that an acidic group as well as an aromatic structure was important in activity against PAI-1.⁶⁰ Reinforcing this, the Rupin study analyzed benzothiophene, benzofuran, and indole-based derivatives and reported findings that also pointed to the importance of an acid functional group and aromatic rings in the structures of PAI-1 inhibitors.⁵⁸ The apparent downside was that the derivatives also exhibited poor solubility and bioavailability and, therefore, were not viable options to inhibit PAI-1 as a drug.

In the same vein, Wyeth later reported an oxadiazolidinedione inhibitor (I-9) against PAI-1 with an IC_{50} of 0.39 μM and further expanded their research to synthesize PAI-749 (I-10).^{52,60} PAI-749 was unique in that it acted on PAI-1 with a dual action mechanism. PAI-749 could bind to PAI-1 and block the tPA active site, thereby preventing the SDS-stable tPA/PAI-1 complex formation. It could also bind to PAI-1 in such a way that it would promote the plasmin-mediated proteolytic degradation of PAI-1. PAI-749 was found to have an IC_{50} value for tPA inhibition of 0.157 μM and an IC_{50} value for uPA inhibition of 0.087 μM . PAI-749 was even found to be effective in the presence of vitronectin and appeared to bind competitively with it.⁶¹ Nonetheless a study performed by Lucking et al. concluded that PAI-749 could in fact not inhibit thrombus formation or increase fibrinolysis *in vitro* or *ex vivo* while tPA was present and, therefore, alongside of its poor pharmacokinetic properties, was not a viable PAI-1 inhibitor for human systems.⁶²



Wyeth subsequently developed PAZ-417 (structure unrevealed), a molecule that was found to reduce A β levels in plasma and in the brain. It had an IC_{50} value against PAI-1 of 0.655 μM and although it seemed to show promise, nothing was published on its clinical results.⁵⁷

With developing technology, another molecule was discovered through high throughput screening. ZK4044 (I-11) was found to be effective against PAI-1 with an IC_{50} value of 0.644 μM . ZK4044 selectively binds to PAI-1 over other serpins and was found to directly inhibit binding of PAI-1 to tPA and uPA. Interestingly, ZK4044 was also discovered to prevent conversion of PAI-1 from active to latent form. However, due to its hydrophobic menthol-based structure, it requires optimization before further pharmacological use.²⁴

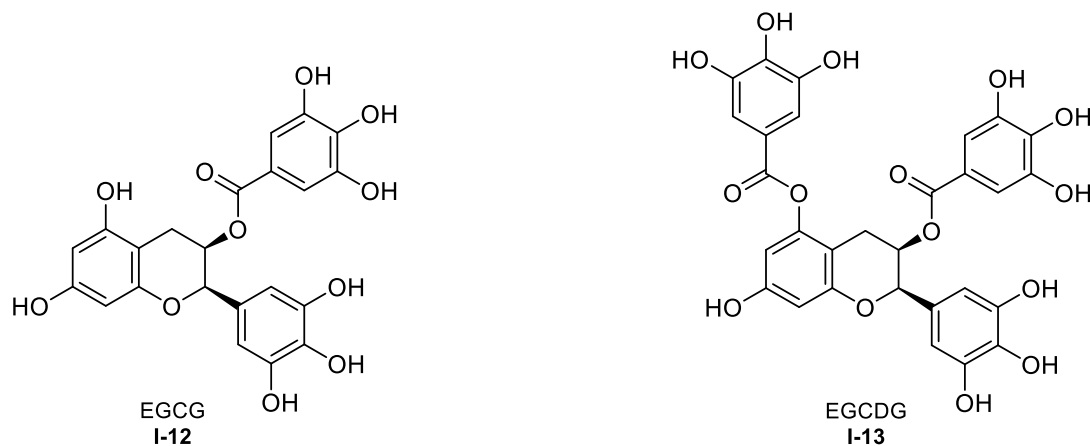


In 2007 our research group began a collaborative effort with that of Professor Daniel Lawrence of the University of Michigan Medical School in order to further advance the discovery and development of novel small molecule inhibitors of PAI-1. With the aid of a high throughput screen of the MicroSource SPECTRUM compound library, Lawrence and his group

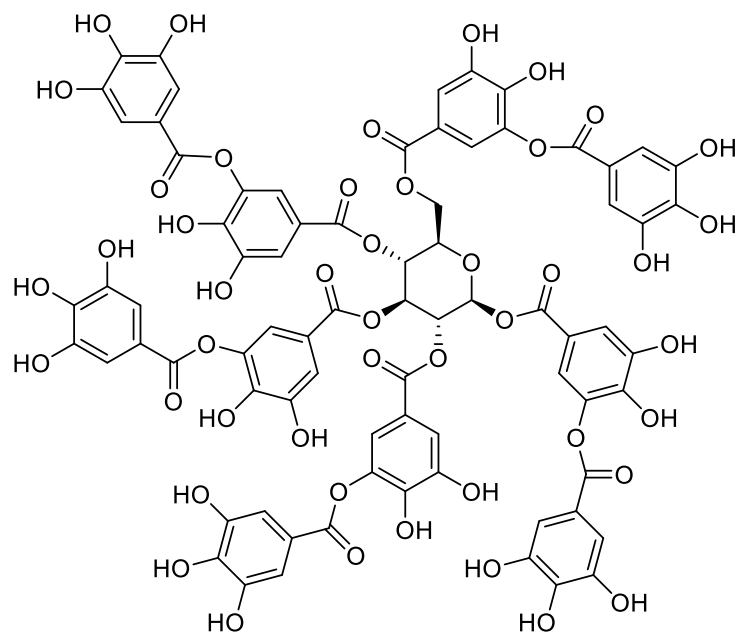
were able to identify a total of 19 varied compounds that displayed activity against PAI-1.

Interestingly, three of these molecules contained galloyl moieties (3,4,5-trihydroxybenzoates).⁵⁶

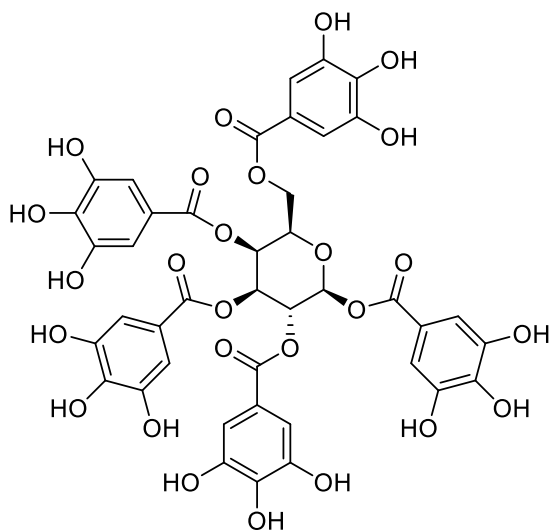
EGCG (I-12) and EGCDG (I-13), each containing three gallate groups, were found to have strong PAI-1 inhibitory activity. However the necessary purification and synthesis methods were deemed too expensive and laborious.



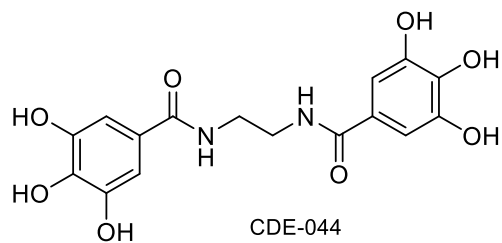
The third, tannic acid (I-14), is a naturally occurring polyphenolic compound whose structure suggests potential PAI-1 activity due to its large number of gallate groups. Although it is a potent PAI-1 inhibitor with an IC_{50} value of 7 nM, it would not make a very successful drug due to its high molecular weight and tendency to form aggregates at micromolar concentrations. Therefore, a second generation of derivatives were synthesized that exhibited enhanced potency of PAI-1 activity by 10-1000 fold over previously reported inhibitors (**Figure 4**).⁵⁶ These new compounds displayed better PAI-1 activity than tiplaxtinin and were able to inhibit the Michaelis-like complex that forms between PAI-1 and tPA/uPA. They were also importantly shown to inhibit vitronectin-bound PAI-1. They were capable of reversibly binding to PAI-1 with high affinity, indicating their IC_{50} values were not time dependent.



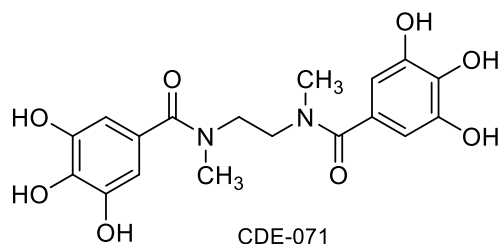
Tannic Acid
 $IC_{50} = 7 \text{ nM}$
I-14



CDE-004
I-15



CDE-044
I-16



CDE-071
I-17

Figure 4. Second generation synthesized compounds

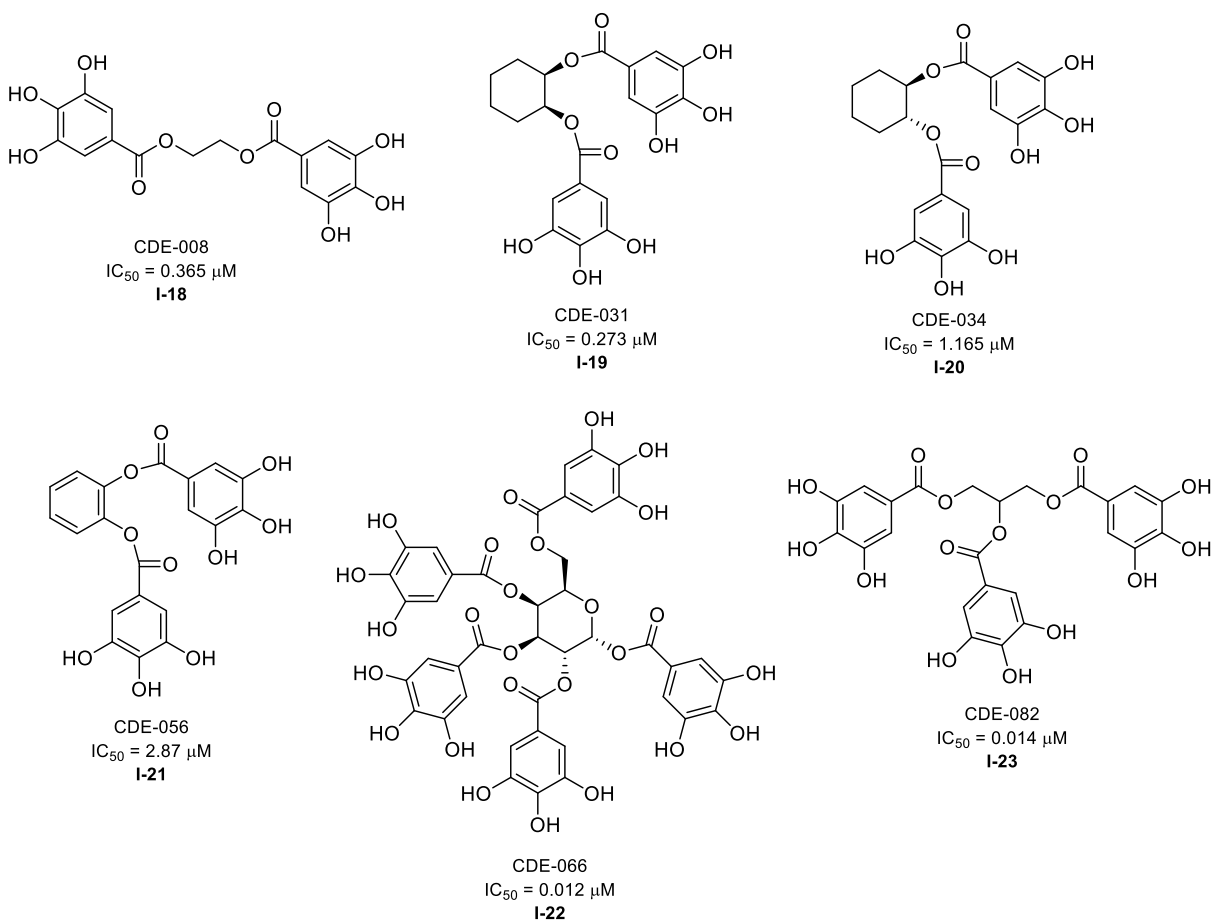


Figure 4 (continued). Second generation synthesized compounds

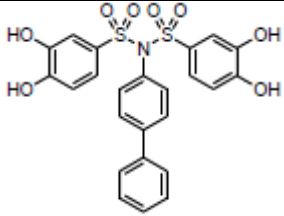
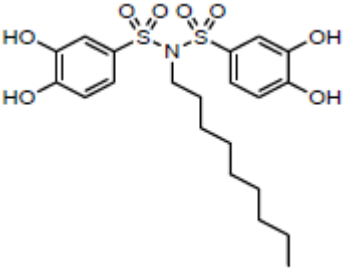
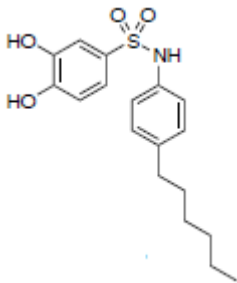
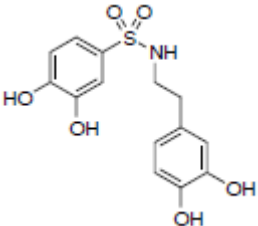
The structures of compounds CDE-004 (I-15) and CDE-066 (I-22) retained many of tannic acid's gallate groups, and their anti-PAI-1 activity in the low nM range spurred further synthesis of molecules with fewer gallate groups to test the effect on activity against PAI-1. A concurrent goal was to investigate the linking unit's role in the molecule's activity. CDE-008 (I-18), CDE-044 (I-16) and CDE-071 (I-17) were synthesized with these factors in mind. However, it was expected that the ester linkages would be susceptible to hydrolysis by esterases as well as by the acidic environment of the stomach. This made *in vivo* testing very limited and ruled out oral administration.⁵⁶ In addition, it was found that this class of compounds did not typically retain activity against PAI-1 in *ex vivo* experiments containing plasma proteins, most likely due

to their ester linkages. On the other hand, those with more galloyl groups seemed to perform better against PAI-1 in plasma.

In an attempt to overcome this issue, the ester linkages were replaced with more stable bis-arylsulfonamides and aryl sulfonamide groups in a series of compounds (**Table 1**). It was found that molecules that contained two sulfonyl groups were most effective against PAI-1,⁶³ that 3,4-dihydroxy substitution gave the lowest IC₅₀ values, and that some non-symmetric inhibitors also proved effective (CDE-187 and 198).⁶³ While these molecules have shown promise and were further investigated by our research group, one of their major setbacks was loss of activity in assays containing plasma.³⁰

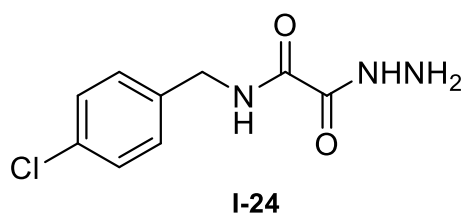
Table 1. Sulfonamide and sulfonimide based inhibitors

CDE Code	Structure	IC ₅₀ Value (μM)
CDE-032		9.45
CDE-119		6134
CDE-132		1384
CDE-135		104
CDE-140		318

CDE-165		0.35
CDE-183		0.18
CDE-187		0.91
CDE-198		0.051

In order to find another lead compound, a second high throughput library screen was performed on a much larger set of molecules maintained by the Center for Chemical Genomics (CCG) at the University of Michigan. This screen discovered two main molecules with anti-PAI-1 activity. Of these, **I-24**, was chosen for further studies due to its low molecular weight, low micromolar IC₅₀ value of 36 μM, and suitability as a framework for synthesizing many derivatives. **I-24** lacks any galloyl groups in exchange for a single benzene ring with a *para*

substituted chlorine, drawing electron density out of the ring. It also includes a highly active hydrazide on its opposite end. We decided that our research group would undertake the challenge of synthesizing a host of analogs to **I-24** in order to better understand the structure activity relationships between various moieties in the compound and PAI-1 inhibition.



References:

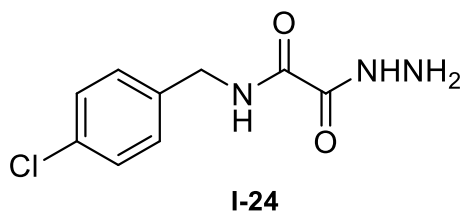
1. Ploplis, V. A. *Curr. Drug Targets* **2011**, *12*, 1782–1789.
2. Simpson, A.J.; Booth, N.A.; Moore, N.R.; Bennett, B. *J. Clin. Pathol.* **1991**, *44*(2): 139-143.
3. McGill, J. B.; Schneider, D. J.; Arfken, C. L.; Lucore, C. L.; Sobel, B. E. *Diabetes* **1994**, *43*, 104–109.
4. Stefansson, S.; Petitclerc, E.; Wong, M. K.; McMahon, G. A.; Brooks, P. C.; Lawrence, D. A. *J. Biol. Chem.* **2001**, *276*, 8135–8141.
5. Bacharach, E.; Itin, A.; Keshet, E. *Proc. Natl. Acad. Sci.* **1992**, *89*, 10686-10690.
6. Pepper, M. S.; Montesano, R.; Mandriota, S. J.; Orci, L.; Vassalli, J. D. *Enzyme & Protein.* **1996**, *49*, 138-162.
7. McMahon. *J. Biol. Chem.* **2001**, *276*, 33964–33968.
8. Folkman, J. *Seminars in Oncology* **2002**, *29*, 15-18.
9. Zetter, B. R. *Annu. Rev. Med.* **1998**, *49*, 407-424.
10. Folkman, J. *Nat. Med.* **1995**, *1*, 27-31.
11. Dewild, M.; Strelkov, S.; Rabijns, A.; Declerck, P. *J. Struct. Biol.* **2009**, *165*, 126-132.
12. Liu, R. M.; van Groen, T.; Katre, A.; Cao, D.; Kadisha, I.; Ballinger, C.; Wang, L.; Carroll, S. L.; Li, L. *Neurobiol. Aging* **2011**, *32*, 1079-1089.
13. Ross, R. *Nature* **1993**, *362*, 801-809.
14. Bini, A.; Fenoglio J.J.; Mesa- Tejada, R.; Kudryk, B.; Kaplan, K.L. *Arteriosclerosis* **1989**, *9*, 109-121.
15. Carmeliet, P.; Stassen, J. M.; Schoonjans, L.; Ream, B.; van den Oord, J. J.; De Mol, M.; Mulligan, R. C.; Collen, D. *J. Clin. Invest.* **1993**, *92*, 2756-2760.
16. Eitzman, D. T.; Westrick, R. J.; Xu, Z.; Tyson, J.; Ginsburg, D. *J. Clin. Invest.* **1996**, *97*, 232-237.
17. Eitzman, D. T.; Westrick, R. J.; Xu, Z.; Tyson, J.; Ginsburg, D. *Blood* **2000**, *96*, 4212-4215.
18. Weisberg, A. D.; Albornoz, F.; Griffin, J. P.; Crandall, D. L.; Elokda, H.; Fogo, A. B.; Vaughan, D. E.; Brown, N. J. *Arterioscler. Thromb. Vasc. Biol.* **2005**, *25*, 365-371.
19. Nicholas, S. B.; Aguiniga, E.; Ren, Y.; Kim, J.; Wong, J.; Govindarajan, N.; Noda, M.; Wang, W.; Kawano, Y.; Collins, A.; Hsueh, W. A. *Kidney Int.* **2005**, *67*, 1297-1307.
20. Eitzman, D. T., Mc Coy, R. D.; Zheng, X.; Fay, W.P.; Shen, T.; Ginsburg, D.; Simon, R. H. *J. Clin. Invest.* **1996**, *97*, 232-237.
21. Ghosh, A. K.; Bradham, W. S.; Gleaves, L. A.; De Taeye, B.; Murphy, S. B.; Covington, J. W.; Vaughan, D. E. *Circulation* **2010**, *122*, 1200-1209.
22. Gils, A.; Declerck, P. *J. Thromb. Haemost.* **2004**, *91*, 425-437.
23. Irving, J. A.; Pike, R. N.; Lesk, A. M.; Whisstock, J. C. *Genome Res.* **2000**, *10*, 1845–1864.
24. Liang, A.; Wu, F.; Tran, K.; Jones, S. W.; Deng, G.; Ye, B.; Zhao, Z.; Snider, R. M.; Dole, W. P.; Morser, J.; Wu, Q. *Thromb. Res.* **2005**, *115*, 341–350.
25. Sawdey, M. S.; Loskutoff, D. J. *J. Clin. Invest.* **1991**, *88*, 1346–1353.
26. Ginsburg, D.; Zeheb, R.; Yang, A.Y. *J. Clin. Invest.* **1986**, *78*, 1673-1680.
27. Loskutoff, D. J.; Linders, M.; Keijer, J. *Biochemistry* **1987**, *26*, 3763-3768.
28. Silverman, G. A.; Bird, P. I.; Carrell, R. W.; Church, F. C.; Coughlin, P. B.; Gettins, P. G.; Irving, J.A.; Lomas, D. A.; Luke, C. J.; Moyer, R. W. *J. Biol. Chem.* **2001**, *276*, 33293-33296.

29. Binder, B. R.; Christ, G.; Gruber, F.; Grubic, N.; Hufnagl, P.; Krebs, M.; Mihaly, J.; Prager, G. W. *Physiological Sciences*. **2002**, *17*, 56-61.
30. Weerakoon, D. Design, Synthesis and Evaluation of Small Molecules as Inhibitors of Plasminogen Activator Inhibitor-1, Eastern Michigan University: Ypsilanti, Michigan, 2014.
31. Ko, C. W.; Wei, Z.; Marsh, R. J.; Armoogum, D. A.; Nicolaou, N.; Bain, A. J.; Zhou, A.; Ying, L. *Mol. BioSyst.* **2009**, *5*, 1025–1031.
32. Lin, Z.; Jiang, L.; Yuan, C.; Jensen, J. K.; Zhang, X.; Luo, Z.; Furie, B. C.; Furie, B.; Andreasen, P. A.; Huang, M. *J. Biol. Chem.* **2011**, *286*, 7027–7032.
33. Ngo, T. H.; Zhou, Y.; Stassen, J. M. *Thromb. Haemost.* **2002**, *88*, 288-93.
34. Mottonen, J.; Strand, A.; Symersky, J.; Sweet, R. M.; Danley, D. E.; Geoghegan, K.F.; Gerard, R. D.; Goldsmith, E.J. *Nature* **1992**, *355*, 270-273.
35. Naessens, D.; Gils, A.; Compernelle, G.; Declerck, P. J. *Thromb. Haemost.* **2003**, *90*, 52-58.
36. Stromqvist, M.; Andersson, J. O.; Bostrom, S.; Deinum, J.; Ehnebom, J.; Enquist, K.; Johansson, T.; Hansson, L. *Protein Expr. Purif.* **1994**, *5*, 309-316.
37. Verhamme, I.; Kvassman, J.O.; Duane Day, D.; Debrock, S.; Vleugels, N.; Declerck, P. J.; Shore, J. D. *J. Biol. Chem.* **1999**, *274*, 17511-17517.
38. Lawrence, D. A.; Olson, S. T.; Palaniappan, S.; Ginsburg, D. *Biochemistry* **1994**, *33*, 3643-3648.
39. Declerck, P. J.; DeMol, M.; Alessi, M. C.; Baudner, S.; Paques, E. P.; Preisser, K. T.; Muller-Berghaus, G.; Collen, D. *J. Biol. Chem.* **1988**, *263*, 15454-15461.
40. Zhou, A.; Huntington, J. A.; Pannu, N.S.; Carrell, R.W.; Read, R.J. *Nat Struct Biol.* **2003**, *10*(7), 541-4.
41. Xu, z.; Balsara, R. D.; Gorlatova, N. V.; Lawrence, D. A.; Castellino, F. J.; Ploplis, V. A. *J. Biol. Chem.* **2004**, *279*, 17914-17920.
42. Minor, K. H.; Peterson, C. B. Plasminogen Activator Inhibitor Type 1 Promotes the Self-Association of Vitronectin into Complexes Exhibiting Altered Incorporation into the Extracellular Matrix. *Journal of Biological Chemistry* **2002**, *277* (12), 10337–10345.
43. Perrie, A. M.; Mac Gregor, I. R.; Booth N. A. *Fibrinolysis* **1993**, *7*, 257-63.
44. Bijmens, A. P.; Gils, A.; Stassen, J. M. *J. Biol. Chem.* **2001**, *276*, 44912-8.
45. Debrock, S.; Declerck, P. J. *Biochim. Biophys. Acta.* **1997**, *1337*, 257-66.
46. Bijmens, A. P.; Gils, A.; Knockaert, I. *J. Biol. Chem* **2000**, *275*, 6375-80.
47. Eitzman, D. T.; Fay, W. P.; Lawrence, D. A. *J. Biol. Chem.* **1995**, *95*, 2416-20.
48. Fay, W. P.; Parker, A. C.; Condrey, L. R.; Shapiro, A. D. *Blood.* **1997**, *90*, 204-208.
49. Fujii, S.; Sawa, H.; Sobel, B. E. *Thromb. Haemost.* **1993**, *70*, 642-647.
50. Bryans, J.; Charlton, P.; Chicarelli-Robinson, I.; Collins, M.; Faint, R.; Latham, C.; Shaw, I. *J. Antithromb.* **1996**, *49*(10), 1014-1021.
51. Charlton, P.; Faint, R.; Barnes, C.; Bent, F.; Folkes, A.; Templeton, D.; Mackie, I.; Machin, S.; Bevan, P. *Fibrinolysis Proteolysis.* **1997**, *11*, 51-56.
52. Gopalsamy, A.; Kincaid, S. L.; Ellingboe, J. W.; Groeling, T. M.; Antrilli, T. M.; Krishnamurthy, G.; Aulabaugh, A.; Friedrichs, G. S.; Crandall, D. L. *Bioorg. Med. Chem. Lett.* **2004**, *14*, 3477-3480.
53. Folkes, A.; Roe, M. B.; Sohal, S.; Golec, J.; Faint, R.; Brooks, T.; Charlton, P. *Bioorg. Med. Chem. Lett.* **2001**, *11*, 2589-2592.
54. Elokdah, H.; Abou-Gharbia, M.; Hennan, J. K.; McFarlane, G.; Mugford, C. P.; Krishnamurthy, G.; Crandall, D. L. *J. Med. Chem.* **2004**, *47*, 3491-3494.

55. Gorlatova, N.V.; Cale, J.M.; Elokdah, H.; Li, D.; Fan, K.; Warnock, M.; Crandall, D.L.; Lawrence, D.A. *J. Biol. Chem.* **2007**, *282*, 9288-9296.
56. Cale, J.M.; Li, S.H.; Warnock, M.; Su, E.J.; North, P.R.; Sanders, K.L.; Puscau, M.M.; Emal, C.D.; Lawrence, D.A. *J. Biol. Chem.* **2010**, *285*, 7892-7902.
57. Crandall, D. L.; Elokdah, H.; Di, L.; Hennen, J. K.; Gorlatova, N. V.; Lawrence, D. A. *J. Thromb. Haemost.* **2004**, *2*, 1422-1428.
58. Rupin, A.; Gaertner, R.; Mennecier, P.; Richard, I.; Benoist, A.; De Nanteuil, G.; Verbeuren, T. J. *Thromb. Res.* **2008**, *122*, 265-270.
59. Bjorquist, P.; Ehnemob, J.; Inghardt, T.; Hansson, L.; Lindberg, M.; Linschoten, M.; Stromqvist, M.; Deinum, J. *Biochemistry* **1998**, *37*, 1227-1234.
60. De Nanteuil, G.; Lila-Ambroise, C.; Rupin, A.; Vallez, M.; Verbeuren, T. J. *Bioorg. Med. Chem. Lett.* **2003**, *13*, 1705-1708.
61. Gardell, S. J.; Krueger, J. A.; Antrilli, T. A.; Elokdah, H.; Mayer, S.; Orcutt, S. J.; Crandall, D. L.; Vlasuk, G. P. *Mol. Pharmacol.* **2007**, *72*, 897-906.
62. Lucking, A. J.; Visvanathan, A.; Philippou, H.; Fraser, S.; Grant, P. J.; Connolly, T. M.; Gardell, S. J.; Feuerstein, G. Z.; Fox, K. A. A.; Booth, N. A.; Newby, D. E. *J. Thromb. Haemost.* **2010**, *8*, 1333-1339.
63. El-Ayache, N. C.; Li, S.; Warnock, M.; Lawrence, D. A.; Emal, C. D. *Bioorg. Med. Chem. Lett.* **2010**, *20*, 966-970.

Chapter II

II-1: Novel Small Molecule Inhibitors of PAI-1



The main goal of my work was to improve the lead molecule's IC_{50} value, as well as to analyze structure activity relationships of various structural features of this PAI-1 inhibitor. I pursued these goals by synthesizing various analogs of **I-24** with variations at three locations: I substituted different groups on the aromatic ring, extended the oxalyl core chain length, and exchanged the hydrazide group on the end of the lead molecule with other moieties (**Figure 5**).

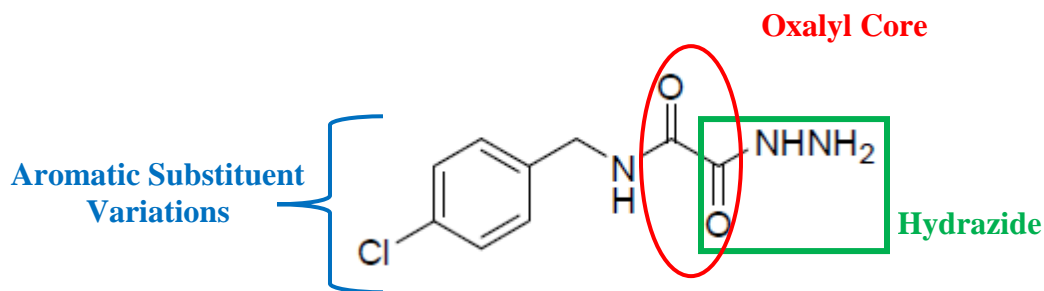
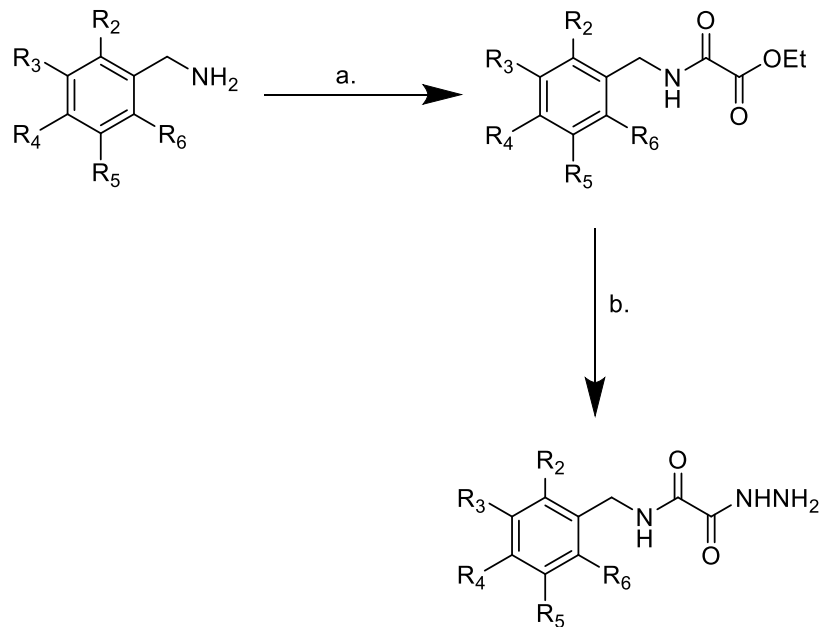


Figure 5. Locations of analogue syntheses

II-2: Aromatic Substituent Variations

My first objective was to vary substituents on the aromatic ring to study their effect on PAI-1 inhibitory activity. **Scheme 1** details the general procedure for synthesizing these analogues. Substituted benzylamines were placed in a solution of pyridine and methylene chloride. To this, ethyl oxalyl chloride was added to form an ester intermediate. This ester was then dissolved in ethanol and treated with hydrazine hydrate to provide the final product to be analyzed for activity versus PAI-1.



Scheme 1. Synthesis of lead molecule analogs from benzene ring substitutions. Reagents and conditions: a. ethyl oxalyl chloride, pyridine, CH₂Cl₂, 0 °C to r.t.; b. hydrazine hydrate, ethanol, r.t.

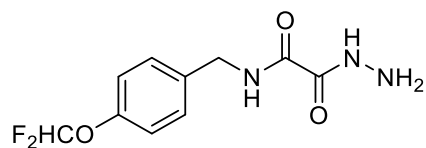
Following synthesis and verification of product via ¹H NMR and ¹³C NMR, all products were tested in Dr. Lawrence's lab for inhibitory activity versus PAI-1. Molecules were tested under two conditions: a simple pH 7.4 buffer with PAI-1 and uPA, and with the addition of 1.5% bovine serum albumin (BSA) to the pH 7.4 buffer. The BSA adds proteins that allow the assay to more closely mimic the physiological conditions of a whole organism. The molecules that were synthesized and their inhibitory assay results are shown in **Table 2**.

Table 2: Oxalyl core benzene ring substituent variations.

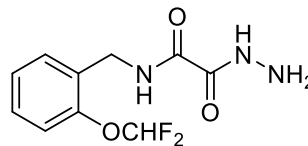
Compound Code Category A	R2	R3	R4	R5	R6	IC ₅₀ (μ M) pH 7.4	IC ₅₀ (μ M) 1.5% BSA
Lead (I-24)	H	H	Cl	H	H	117	54
CDE-486	H	H	OCHF ₂	H	H	>3000	324
CDE-487	H	H	H	H	OCHF ₂	>3000	>3000
CDE-488	F	CF ₃	H	H	H	387	157
CDE-492	F	CH ₃	H	H	F	3188	1274
CDE-493	F	F	F	H	H	809	267
CDE-494	Cl	F	H	H	F	>3000	>3000
CDE-495	H	CF ₃	F	H	H	247	99.6
CDE-496	H	H	<i>i</i> Pr	H	H	976	205
CDE-497	H	H	N(CH ₃) ₂	H	H	>3000	469
CDE-498	H	H	CH ₂ CH ₃	H	H	2679	134
CDE-499	H	CH ₃	F	H	H	268	90.7
CDE-268 ^a	H	OCF ₃	H	H	H	131	109

^aCompound synthesized by Naga Guntaka. Substituent locations shown in **Scheme 1**.

Analysis of the data acquired for the analogues I synthesized suggests that an electronegative group in the *para* (R4) position on the ring leads to lower IC₅₀ values. For example, when comparing CDE-486, with the substituent in the *para* position, and CDE-487, where it is meta, CDE-486 has a significantly lower IC₅₀ in BSA.

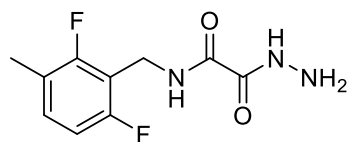


CDE-486
IC₅₀ = 324 μM

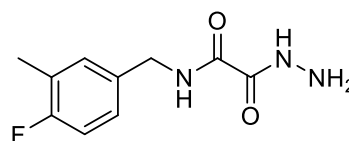


CDE-487
IC₅₀ = >3000 μM

A similar parallel is seen between CDE-492 and CDE-499. The inclusion of a fluorine atom in the *para* (R4) position of CDE-499 seems to have drastically improved its inhibition capability. It should be noted that the fluorine in the second position on the ring has been removed in CDE-499, which may have some effect in the change of IC₅₀ values, as many compounds without an electron withdrawing group at that position show a trend of possessing lower IC₅₀ values.

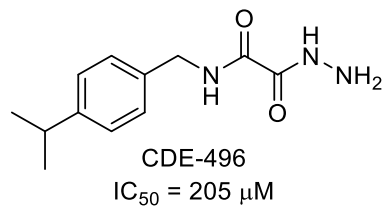
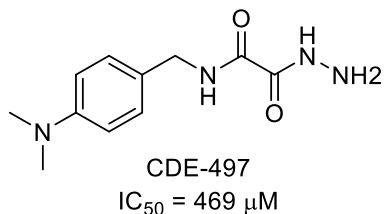


CDE-492
IC₅₀ = 1274 μM

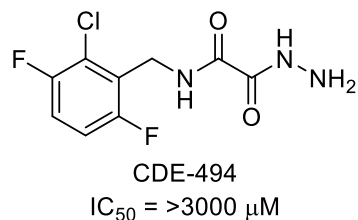
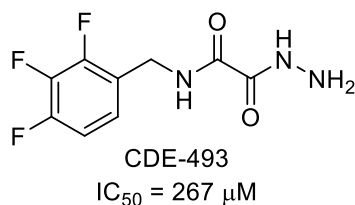


CDE-499
IC₅₀ = 90.7 μM

The data indicates a correlation between lower IC₅₀ values and the presence of substituents in the *para* position, as well as a preference for electron withdrawing groups at that position, as opposed to electron donating groups. CDE-497 was synthesized with an electron donating tertiary nitrogen at the *para* position; while measurable inhibition does occur within the test range, it is noticeably worse than previous molecules that contain electron withdrawing groups at that position. In the same sense, CDE-496, containing an isopropyl group, which is far less withdrawing than the groups on some of the other molecules synthesized, is also seen to have a more effective inhibitory effect than that of CDE-497.



It is interesting to note that there is a correlation between a substituent on the *ortho* (R6) position and a decreased inhibitory effect. CDE-493 and CDE-494 contain similar electronegative substituents, with the main difference being the position of the third substituent. CDE-493 contains a *para* (R4) substituent while CDE-494 has a second *ortho* (R6) substituent. This difference results in a significant decrease in inhibitory effect for CDE-494. This is also seen in the previous comparison of CDE-486 and CDE-487, as well as CDE-492, which has the third least effective IC₅₀ value.



II-3: Extension of Core Chain Length Analogues

The second portion of my research was to determine the effect of extending the two - carbon oxalyl core to the three and four carbon malonyl and succinyl cores, respectively (**Figure 6**). In these cases only one benzyl amine was used for all syntheses. A trifluoromethoxy group on the *meta* (R3) position on the ring was utilized. This was done in an effort to keep the aromatic ring substitution consistent, as well as benefit from the previous use of this benzyl amine in the syntheses of similar molecules. In these syntheses, the hydrazide group was modified to match

other molecules with the original oxalyl core, where the molecules I synthesized and their inhibitory assay results are listed in **Table 3** and **Table 4**; and their original counterparts are displayed in **Table 5**.

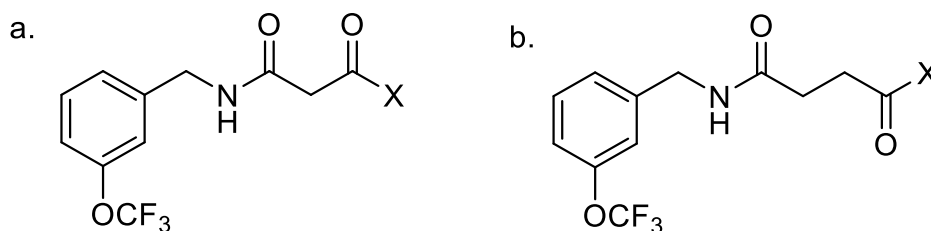
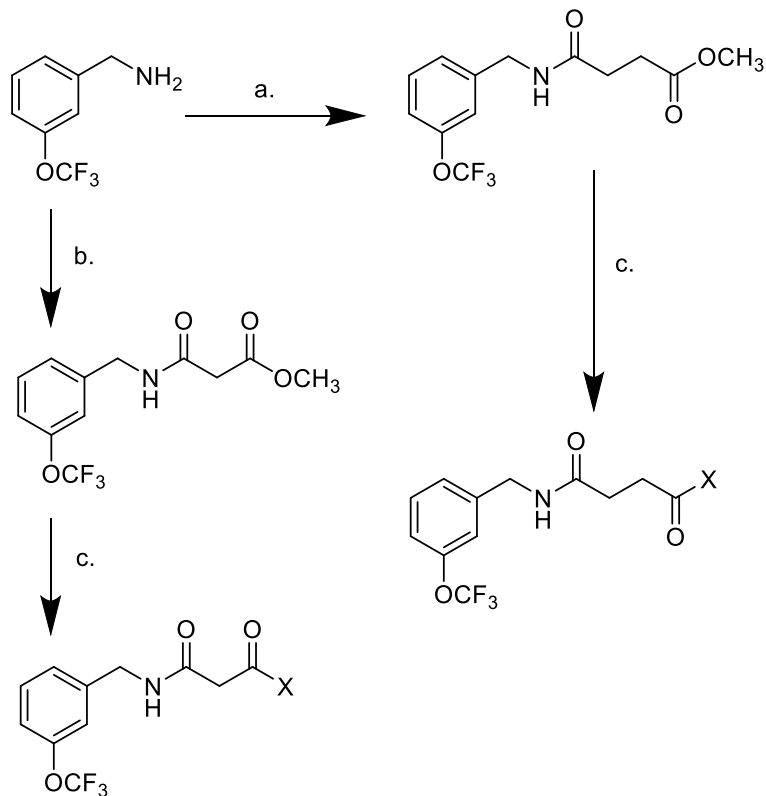


Figure 6. Malonyl (a) and Succinyl (b) cores

The intermediate esters leading to CDE compounds 501, 502, 503, 504, 505, 506, 509, 511, 521, 522, 523, and 524 were synthesized in the same manner as previous benzyl amine analogues. 3-Trifluoromethoxy benzyl amine was added to a solution of methylene chloride and pyridine. Methyl malonyl chloride or methyl succinyl chloride was added dropwise to provide the resulting ester. The esters then underwent the appropriate reactions in order to afford the final compounds. CDE-502 and 511 were treated with hydrazine hydrate; CDE-503 and 521 were subjected to aqueous base; CDE-504, 505, 522, and 523 were reacted with a beta amide ester salt under standard peptide-coupling conditions; CDE-506 and 524 were treated with ammonia in methanol (7 N) (**Scheme 2**).



Scheme 2. Syntheses of malonyl & succinyl compounds with varying end moieties. Reagent and conditions. (a): methyl malonyl chloride, pyridine, CH_2Cl_2 , $0\text{ }^\circ\text{C}$ to rt. (b): methyl succinyl chloride, pyridine, CH_2Cl_2 , $0\text{ }^\circ\text{C}$ to rt. (c): CDE-502 and CDE-511: hydrazine hydrate, EtOH; 503, 521: aq. NaOH (5M), EtOH; CDE-504, 522: 2-amino-1-pyrrolidin-1-yl-ethanone hydrochloride, HOBt · H_2O , DMF, N-methylmorpholine, H_2Cl_2 , EDC · HCl; CDE-505, 523: 2-amino-1-morpholino-1-ethanone hydrochloride, HOBt · H_2O , DMF, N-methylmorpholine, H_2Cl_2 , EDC · HCl; CDE-506 and CDE-524: ammonia in methanol, EtOH.

Table 3. Malonyl-based compounds.

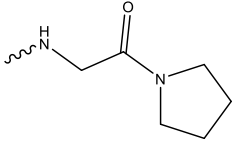
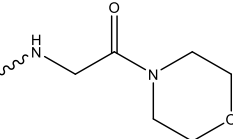
Compound Code	X	IC ₅₀ (μM) pH 7.4	IC ₅₀ (μM) 1.5% BSA
CDE-509	OCH ₃	>3000	>3000
CDE-511	NHNH ₂	>3000	>3000
CDE-521	OH	721	>3000
CDE-522		>3000	>3000
CDE-523		>3000	>3000
CDE-524	NH ₂	139	>3000

Table 4. Succinyl-based Compounds.

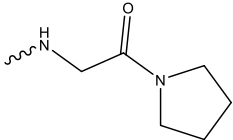
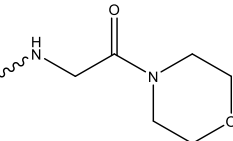
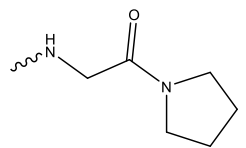
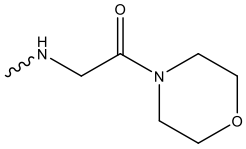
Compound Code Category A	X	IC ₅₀ (μM) pH 7.4	IC ₅₀ (μM) 1.5% BSA
CDE-501	OCH ₃	>3000	1383
CDE-502	NHNH ₂	2017	801
CDE-503	OH	>3000	>3000
CDE-504		948	836
CDE-505		4273	2402
CDE-506	NH ₂	921	3298

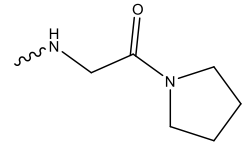
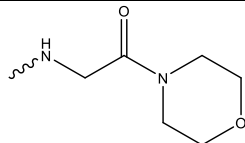
Table 5. Previously synthesized inhibitors.

Compound Code	X	IC ₅₀ (μM) pH 7.4	IC ₅₀ (μM) 1.5% BSA
CDE-471 ^b	NH ₂	421	156
CDE-507 ^a		>3000	>3000
CDE-489 ^a		>3000	2374

Synthesized by: ^aJen Corker, ^bRaKeenja Fluellen.

The results seen in **Table 6** give an interesting insight into the effect of core chain length on the results of the bio assays for this set of molecules. It was hypothesized that there would be a correlation between core length and activity, with one length consistently producing better results than the others. However, that is not the case here. The only consistent result is that molecules with the malonyl core have no activity when in a protein system. This could be due to the atypically acidic C-H bonds on the carbon chain being more susceptible to deprotonation and, therefore, the possible creation of unfavorable interactions with other proteins than those of the succinyl chain protons (the oxalyl chain contains no acidic protons between carbonyls). It is particularly intriguing that even the hydrazide extension on the malonyl core has no activity when every other assay has shown the hydrazide group to produce a significant increase in inhibitory effect.

Table 6. Direct comparison of varying core length inhibitors.

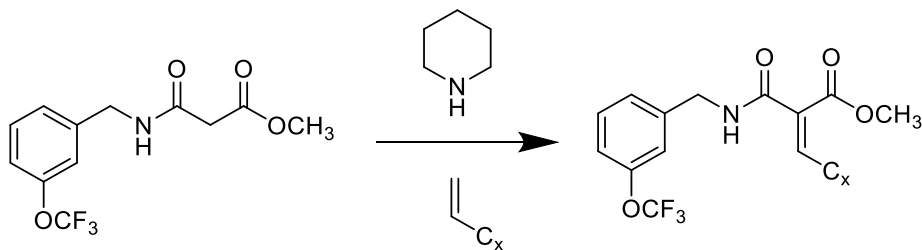
X	Oxalyl IC ₅₀ (μM)		Malonyl IC ₅₀ (μM)		Succinyl IC ₅₀ (μM)	
	pH 7.4	1.5% BSA	pH 7.4	1.5% BSA	pH 7.4	1.5% BSA
OCH ₃	-	-	>3000	>3000	>3000	1383
NHNH ₂	131	109	>3000	>3000	2017	801
OH	-	-	721	>3000	>3000	>3000
	>3000	>3000	>3000	>3000	948	836
	>3000	2374	>3000	>3000	4273	2402
NH ₂	421	156	139	>3000	921	3298

The oxalyl-based inhibitors exhibit better activity than either of the malonyl or succinyl compounds; however, the compound containing the morpholine ring has nearly the same IC₅₀ as the succinyl compound, offsetting the trend. Future research could explore further extension of the core in order to assess the inhibitory effect of chain length, as well as other various end moieties.

II-4: Alpha-Beta Unsaturated Malonyl Derivatives

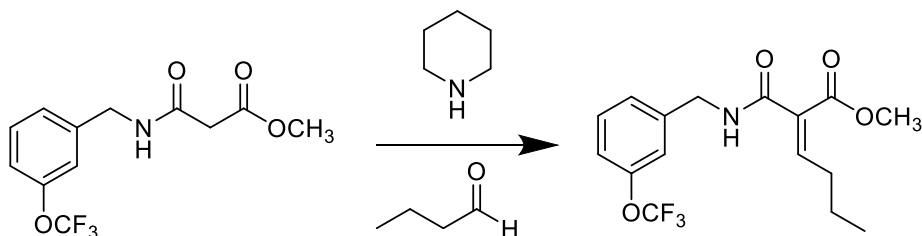
In an effort to increase our understanding of the relationship of structure to inhibition activity, our group is synthesizing an increasingly diverse set of molecules. One of the benefits of extending the core length from our lead molecule to a malonyl core is the ability to utilize the alpha-carbon at each carbonyl as a reactive center for new reactions. I focused on employing a

Knoevenagel reaction, which converts the sp^3 -hybridized carbon at the carbonyl position to an sp^2 -hybridized carbon bound to an additional group. In a microwave tube, I added an aldehyde of choice and piperidine to the previously synthesized malonyl ester (CDE-509). Later syntheses involved the addition of ethyl alcohol as a solvent. The mixture was then subjected to microwave irradiation at 100 °C for 7.5 minutes, followed by an acidic workup (**Scheme 3**).



Scheme 3. Synthesis of alpha-beta unsaturated malonyl derivatives. Reagents & conditions: Piperidine (0.25 eq.), various aldehyde (5 eq.). Microwave irradiation at 250W, 100 °C, 7.5 minutes, no stirring. Later syntheses involved the addition of EtOH as solvent.

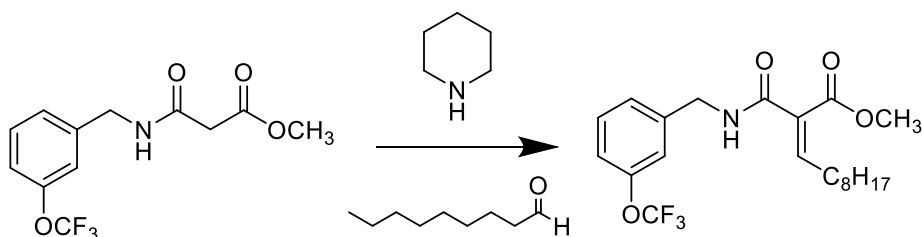
The first attempt was made using butyraldehyde (**Scheme 4**). Preliminary TLC results suggested contamination by side reactions so the product was purified by column chromatography. Post column TLC staining revealed persistent contamination. Preliminary $^1\text{H-NMR}$ indicated a lack of product as well as too many side products to warrant further pursuit. This first attempt was therefore abandoned and a second aldehyde was tried.



Scheme 4. Synthesis of alpha-beta unsaturated malonyl derivative using butyraldehyde. Reagents & conditions: Piperidine (0.25 eq.), butyraldehyde (5 eq.) Microwave irradiation at 250W, 100°C, 7.5 minutes, no stirring.

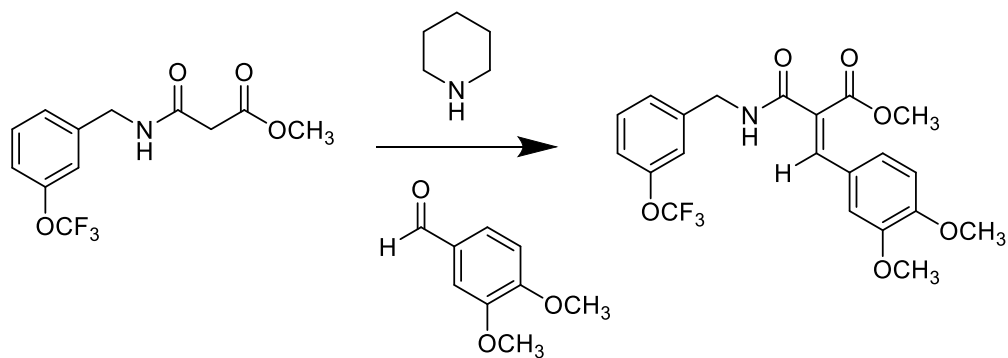
Nonanal was used in an attempt to drive the reaction forward in a more stereo-selective manner due to its long aliphatic chain while keeping the chemistry similar (**Scheme 5**). In the

same way, the aldehyde was added to a microwave tube with piperidine and the starting malonyl ester, then placed in the microwave at 100 °C for 7.5 minutes. Following an acid workup, a column was run in 1% ethyl acetate:hexanes. ¹H-NMR analysis of the resulting separated compounds was inconclusive, and therefore, further TLC staining was performed. Again, this revealed multiple, previously unseen “spots”, and therefore, any further attempts at purification were dismissed.

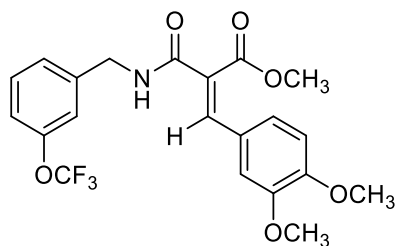


Scheme 5. Synthesis of alpha-beta unsaturated malonyl derivative using nonanal. Reagents & conditions: Piperidine (0.25 eq.), nonanal (5 eq.) Microwave irradiation at 250W, 100 °C, 7.5 minutes, no stirring.

A third attempt at making the desired Knoevenagel reaction proceed correctly was via the use of veratraldehyde (**Scheme 6**). This aldehyde was chosen due to its bulky aromatic group, with hopes that its steric bulk would help drive the reaction towards selectively producing a single isomer. CDE-512 was obtained after workup and a column run in 40% ethyl acetate:hexanes. 2D NMR techniques were then utilized to verify that the *Z* isomer of CDE-512 was the nearly exclusive product (**I-25**).



Scheme 6. Synthesis of alpha-beta unsaturated malonyl derivative using veratraldehyde. Reagents & conditions: Piperidine (0.25 eq.), veratraldehyde (5 eq.) Microwave irradiation at 250W, 100 °C, 7.5 minutes, no stirring.



I-25
CDE-512
IC₅₀ = >3000 μM

1D ¹H-NMR, 1D ¹³C-NMR, COSY, HMQC, and NOESY were used to determine the stereochemistry of CDE-512. Evidence of the exclusive formation of the *Z* isomer was provided mostly by the interactions in the NOESY spectrum of the amide hydrogen solely with its neighboring benzylic hydrogens (**Figure 7**). No other spatial interactions were observed, had the *E* isomer been present, it would likely have shown an interaction between the amide hydrogen and the second aromatic ring.

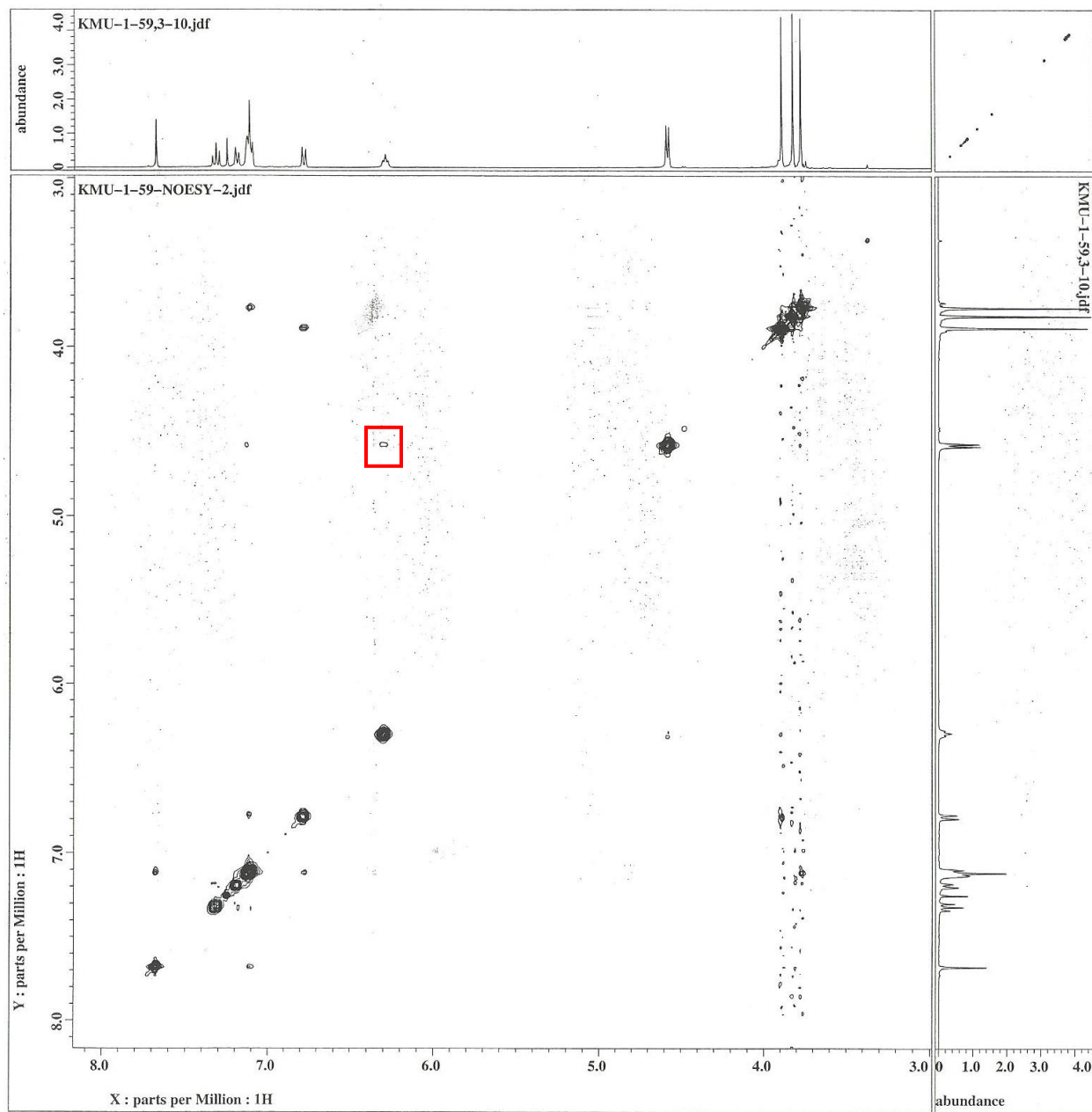
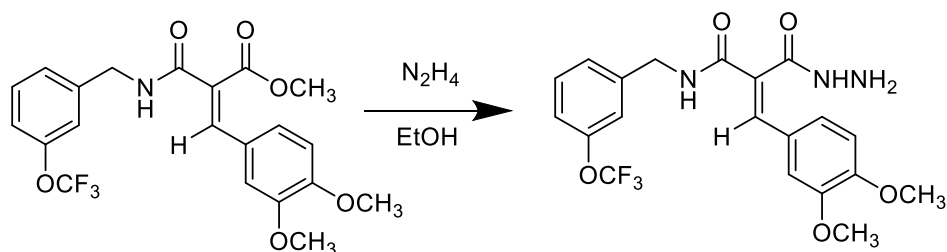


Figure 7. NOESY data of CDE-512. Red box indicates interaction between amide hydrogen & benzylic protons. Lack of any other interactions gives evidence of *Z* isomer.

It may be argued that if CDE-512 were in the *Z* conformation we would see interactions between the vinylic hydrogen and the hydrogen on the amine, which was not observed. This may be due to a lack of specificity in the experiment or these hydrogens being too far away to have any interactions while in the *Z* conformation. Molecular modeling suggests that the amide

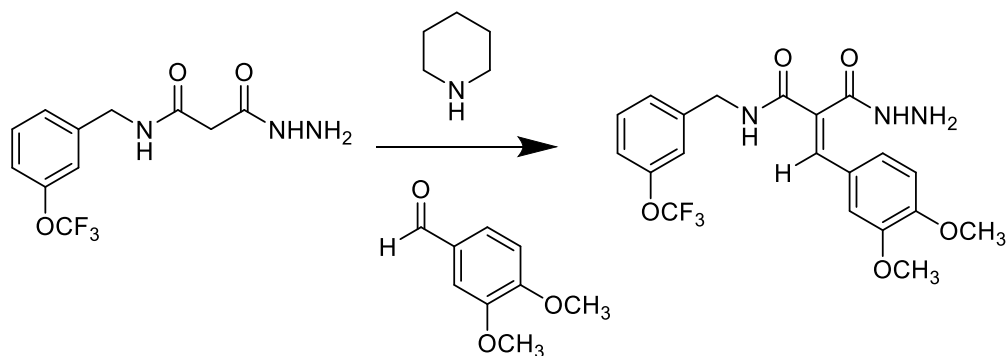
hydrogen could be pointed away from the vinylic proton which also may explain the lack of interaction between the two.

We suspected that CDE-512 would show little activity versus PAI-1 due to its lack of a hydrazide group. However, we were surprised by an almost complete lack of any activity, even in very concentrated amounts (3000 μM). Formation of the hydrazide analog was then attempted using previously-detailed methods (**Scheme 7**). Hydrazine hydrate was added to a solution of CDE-512 in ethanol. Through multiple TLC and column runs, it was determined that no desired hydrazide product was formed and we decided to undertake another method.



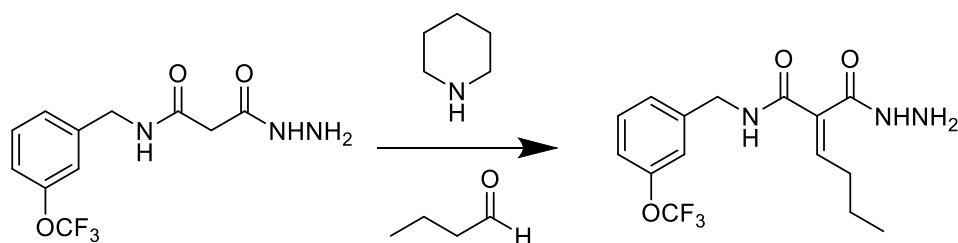
Scheme 7. Formation of hydrazide from α,β -unsaturated malonyl compound. Reagents & conditions: CDE-512 (1 eq.), hydrazine hydrate (2 eq.), ethanol, 24 hours, r.t.

I attempted to synthesize the desired product by subjecting the previously synthesized malonyl hydrazide (CDE-511) in place of the ester (CDE-509) to the Knoevenagel reaction (**Scheme 8**). In a microwave tube, the malonyl hydrazide was combined with 0.25 eq of piperidine, 5 eq of veratraldehyde and 1 mL of EtOH and the reaction mixture was subjected to the same conditions as before. A number of different species were identified via TLC and a column was run to isolate the unidentified products. The ^1H NMR spectrum was inconclusive as to the identity of the products, and therefore, we performed a second synthesis in an effort to obtain the desired products.



Scheme 8. Alternate synthesis for the formation of hydrazide malonyl compound using veratraldehyde. Reagents & conditions: CDE-511 (1 eq.), Piperidine (0.25 eq.), veratraldehyde (5 eq.), ethanol (2 mL). Microwave irradiation at 250W, 100 °C, 7.5 minutes, stirring.

In the same manner as before, I added the malonyl hydrazide to a microwave tube with piperidine, EtOH and butyraldehyde (**Scheme 9**). I used butyraldehyde again despite the previous lack of success because it is a much easier molecule to identify via NMR. In particular, I was looking for the absence of carbonyl alpha protons as well as the presence of a single vinylic proton, which could be easily masked by veratraldehyde in an impure sample. The resulting product was triturated with diethyl ether and a white granular solid was obtained. After drying under vacuum, the sample was subjected to $^1\text{H-NMR}$. We found a near 1:1 ratio of *E* : *Z* isomers; however carbonyl alpha protons were still present near 3.1 ppm and 3.4 ppm. This led me to the conclusion that I had formed the hydrazone instead (**Figure 8**).



Scheme 9. Alternate synthesis for the formation of hydrazide malonyl compound using butyraldehyde. Reagents & conditions: CDE-511 (1 eq.), Piperidine (0.25 eq.), butyraldehyde (5 eq.), ethanol (2 mL). Microwave irradiation at 250W, 100 °C, 7.5 minutes, stirring.

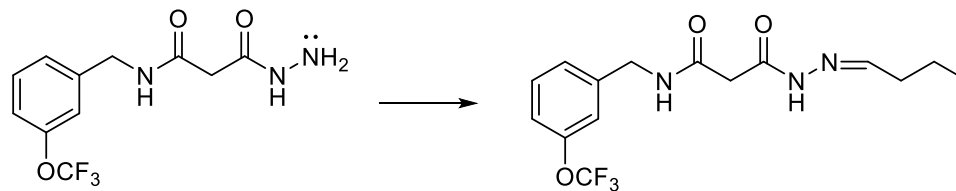


Figure 8. Hydrazone butyraldehyde product reaction

The same analysis was applied to the previously observed veratraldehyde/hydrazide ^1H -NMR. Two singlet peaks from protons alpha to the carbonyls in isomers of the undesirable hydrazone product were identified (**Figure 9**). As a consequence of these results and due to additional impurities, the synthesis of this compound was not pursued further.

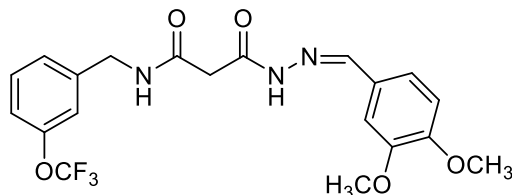
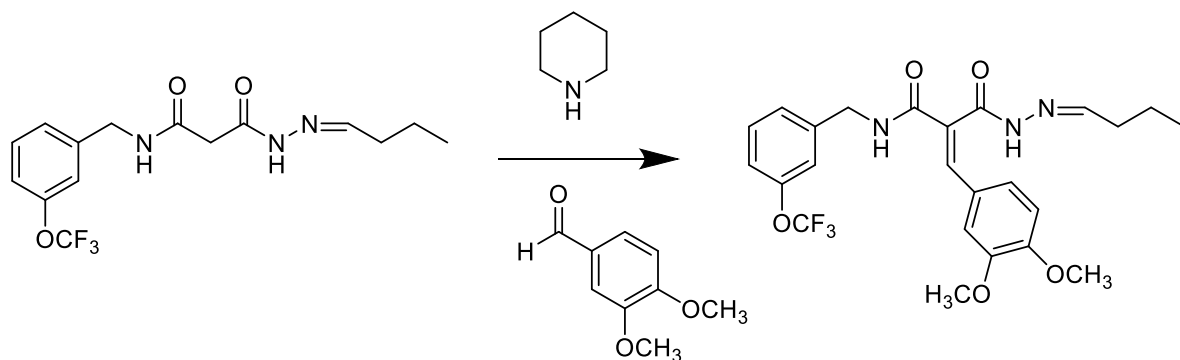


Figure 9. Hydrazone product of veratraldehyde

However, the butyraldehyde hydrazone isomers were of higher purity, and we could perform further attempts to obtain the desired hydrazide product. I attempted to add the veratraldehyde to the originally intended position, hoping that I could reverse the formation of the hydrazone back to the hydrazide following the successful addition of veratraldehyde to the compound (**Scheme 10**). I exposed the hydrazone with the common reagents and veratraldehyde to microwave irradiation as detailed above.



Scheme 10. Synthesis of hydrazone with veratraldehyde. Reagents & conditions: Piperidine (0.25 eq.), veratraldehyde (5 eq.), ethanol (3 mL). Microwave irradiation at 250W, 100 °C, 7.5 minutes, stirring.

Following an acidic workup, TLC was analyzed and it was found that no reaction had taken place. At this point I had a near homogenous solid of starting hydrazone and veratraldehyde, and therefore, decided to try one last reaction with what little materials I had left.

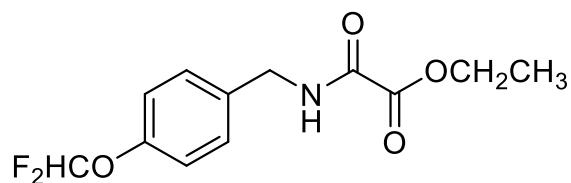
The recovered starting materials from **Scheme 10** were dissolved in EtOH and 4 drops of glacial acetic acid were added. The sample underwent microwave irradiation for 35 minutes, followed by an acid workup as well as a trituration following preliminary NMR. This reaction did not proceed and only miniscule amounts of starting material remained. In the future it could be beneficial to revisit this reaction path. We have observed that the acidic protons in the carbon chain of the other malonyl-based compounds are likely the cause of instability in protein assays. Minor alterations at this site could lead to more potent inhibitors as both the terminal alcohol and amine compounds had moderate inhibition in pH 7.4 buffer. If those compounds could be stabilized, it would be advantageous to test their inhibitory effects in a protein assay.

II-5: Conclusions

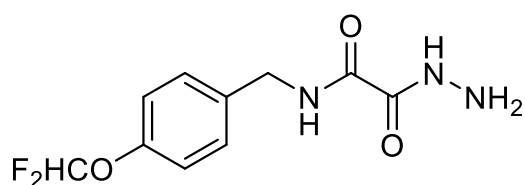
The objective of my research was to synthesize novel small molecules as inhibitors of plasminogen activator inhibitor-1. I synthesized a series of compounds that can be added to a small library of analogues based around the lead molecule, **I-24**. I varied three aspects of the

structure of these compounds. First I altered the nature and position of substituents to the benzene ring while keeping the rest of the molecule the same. I found that there is a positive correlation between inhibitory effect and the presence of an electronegative group at the *para* (R4) position. In addition, a substituent at the *ortho* (R2 or R6) position tends to weaken the inhibitory effect. The second structural modification was to extend the carbon core of the lead molecule and the third modification was to remove and substitute the hydrazine end. Results from these two modifications varied, but it is clear that the three carbon chain malonyl molecules are significantly less effective than the two carbon oxalyl or four carbon succinyl molecules.

Experimental Methods & Data

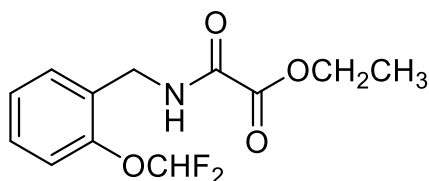


Ethyl 2-((4-(difluoromethoxy)benzyl)amino)-2-oxoacetate (KMU-1-1): To a solution of 4-(difluoromethoxy)benzylamine (0.265 mL, 1.83 mmol) and pyridine (0.30 mL, 3.66 mmol) in 2.0 mL of CH₂Cl₂ stirred in an ice bath, ethylchlorooxacetate (0.21 mL, 1.92 mmol) was added dropwise. The reaction was allowed to stir for one hour. The reaction mixture was then diluted with 30 mL ethyl acetate and washed with 2 × 25 mL of 0.2N HCl, followed by 2 × 25 mL sat. aqueous NaHCO₃. The organic phase was then dried with anhydrous MgSO₄, filtered and concentrated to provide 335.0 mg (67.1%) of the pale yellow solid. ¹H-NMR (CDCl₃, 400 MHz) δ 7.52 (bs, 1H), 7.52 (bs, 1H), 7.27 (d, *J*=8.7 Hz, 2H), 7.05 (d, *J*=8.7 Hz, 2H), 6.47 (t, *J*=6.4 Hz, 2H), 4.29 (q, *J*=7.32 Hz, 2H), 1.34 (t, *J*=6.88 Hz, 3H).

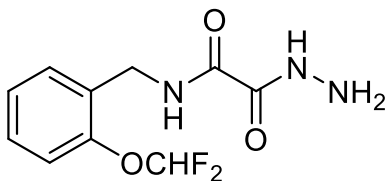


N-(4-(difluoromethoxy)benzyl)-2-hydrazinyl-2-oxoacetamide (CDE-486): A solution of **KMU-1-1** (157.1 mg, 0.549 mmol) and hydrazine hydrate (0.068 mL, 1.098 mmol, ~50% in H₂O) in 4 mL ethanol was stirred for one hour at room temperature. The amorphous solid was filtered and dried under high vacuum to provide 305.0 mg (quantitative yield) of **CDE-486** as an off-white solid. ¹H NMR (DMSO-*d*₆, 400 MHz) δ 10.00 (bs, 1H), 9.25 (t, *J*=5.9 Hz, 1H), 7.17 (dd, *J*=8.7 Hz, 75.6 Hz, 4H), 7.15 (t, *J*=74.7 Hz, 1H), 4.50 (bs, 2H), 4.25 (d, *J*=6.44 Hz, 2H).

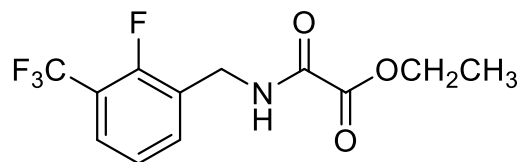
^{13}C NMR (DMSO- d_6 , 100 MHz) δ 160.35, 158.55, 150.36, 136.44, 129.57, 119.26, 116.92 (t, $J=256.5$ Hz), 40.23; HRMS, DART calcd. for $\text{C}_{10}\text{H}_{11}\text{F}_2\text{N}_3\text{O}_3$ [$\text{M}+\text{H}^+$] 260.08467, found: 260.08401.



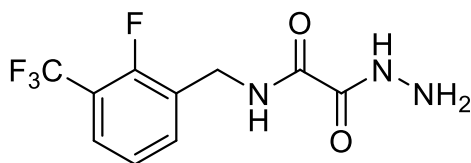
Ethyl 2-((2-(difluoromethoxy)benzyl)amino)-2-oxoacetate (KMU-1-3): The procedure for the synthesis of **KMU-1-1** was followed, substituting 4-(difluoromethoxy)benzylamine for 2-(difluoromethoxy)benzylamine which gave 471.2 mg (94.4%) of **KMU-1-3** as a yellow solid. ^1H NMR (CDCl_3 , 400 MHz) δ 7.80 (m, 5H), 6.58 (t, $J=73.7$ Hz, 1H), 4.56 (d, $J=5.96$ Hz, 2H), 4.33 (q, $J=7.32$ Hz, 2H), 1.37 (t, $J=7.32$ Hz, 3H).



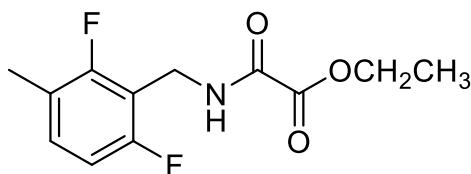
N-(2-(difluoromethoxy)benzyl)-2-hydrazinyl-2-oxoacetamide (CDE-487): A solution of **KMU-1-3** (124.7 mg, 0.456 mmol) and hydrazine hydrate (0.058 mL, 0.912 mmol, ~50% in H_2O) in 4 mL ethanol was stirred for one hour at room temperature. The amorphous solid was filtered and dried under high vacuum to provide 68.5 mg (58.1%) of **CDE-487** as a white solid. ^1H NMR (DMSO- d_6 , 400 MHz) δ 10.04 (bs, 1H), 9.13 (t, $J=6$ Hz, 1H), 7.20 (m, 5H), 4.51 (bs, 2H), 4.32 (d, $J=6$ Hz, 2H). ^{13}C NMR (DMSO- d_6 , 100 MHz) δ 160.54, 158.41, 148.98, 129.96, 129.08, 128.95, 125.81, 118.86, 117.13 (t, $J=257.4$ Hz), 37.41; HRMS, DART calcd. for $\text{C}_{10}\text{H}_{11}\text{F}_2\text{N}_3\text{O}_3$ [$\text{M}+\text{H}^+$] 260.08467, found: 260.08301.



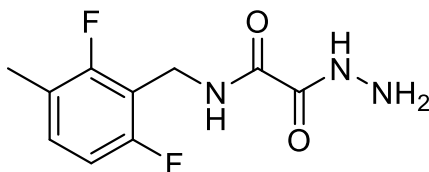
Ethyl 2-((2-fluoro-3-(trifluoromethyl)benzyl)amino)-2-oxoacetate (KMU-1-4): The procedure for the synthesis of **KMU-1-1** was followed, substituting 4-(difluoromethoxy)-benzylamine for 2-fluoro-3-(trifluoromethyl)benzylamine which gave 487.9 mg (91.0%) of **KMU-1-4** as a white solid. ^1H NMR (CDCl_3 , 400 MHz) δ 7.57 (m, 3H), 7.21 (t, $J=7.8$ Hz, 1H), 4.6 (d, $J=6.4$ Hz, 2H), 4.34 (q, $J=7.4$ Hz, 2H), 1.37 (t, $J=7.3$ Hz, 3H).



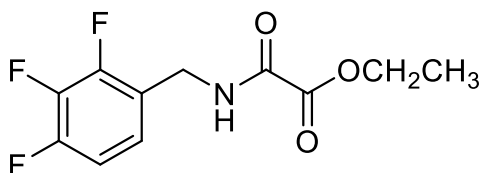
N-(2-fluoro-3-(trifluoromethyl)benzyl)-2-hydrazinyl-2-oxoacetamide (CDE-488): A solution of **KMU-1-4** (116.4 mg, 0.397 mmol) and hydrazine hydrate (0.049 mL, 0.794 mmol, ~50% in H_2O) in 4 mL ethanol was stirred for one hour at room temperature. The amorphous solid was filtered and dried under high vacuum to provide 50.3 mg (45.7%) of **CDE-488** as a white solid. ^1H NMR ($\text{DMSO}-d_6$, 400 MHz) δ 10.06 (bs, 1H), 9.33 (t, $J=6.4$ Hz, 1H), 7.61 (dt, $J=6.9$ Hz, $J=22.9$ Hz, 2H), 7.34 (t, $J=7.8$ Hz, 1H), 4.51 (d, $J=4.1$ Hz, 2H), 4.39 (d, $J=6$ Hz, 2H). ^{13}C NMR ($\text{DMSO}-d_6$, 100 MHz) δ 160.63, 158.25, 157.20 (d, $J=254.6$ Hz), 134.97 (d, $J=4.8$ Hz), 127.9 (d, $J=13.4$ Hz), 126.48 (d, $J=4.8$ Hz), 125.26 (d, $J=3.8$ Hz), 123.25 (q, $J=269.8$ Hz), 116.9 (m), 36.19 (d, $J=4.8$ Hz); HRMS, DART calcd. for $\text{C}_{10}\text{H}_9\text{F}_4\text{N}_3\text{O}_2$ [$\text{M}+\text{H}^+$] 280.07090, found: 280.07199.



Ethyl 2-((2,6-difluoro-3-methylbenzyl)amino)-2-oxoacetate (KMU-1-7): The procedure for the synthesis of **KMU-1-1** was followed, substituting 4-(difluoromethoxy)-benzylamine for 2,6-difluoro-3-methylbenzylamine which gave 435.8 mg (92.7%) of **KMU-1-7** as an off-white solid. ^1H NMR (CDCl_3 , 400 MHz) δ 7.31 (bs, 1H), 7.1 (q, $J=8.7$ Hz, 1H), 6.8 (t, $J=8.7$ Hz, 1H), 4.6 (d, $J=6$ Hz, 2H), 4.32 (q, $J=7.3$ Hz, 2H), 2.23 (t, $J=0.9$ Hz, 3H), 1.37 (t, $J=6.9$ Hz, 3H).

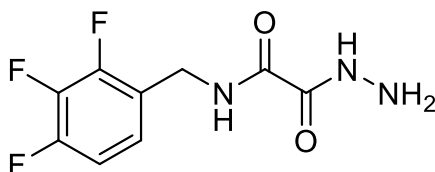


N-(2,6-difluoro-3-methylbenzyl)-2-hydrazinyl-2-oxoacetamide (CDE-492): A solution of **KMU-1-7** (152.2 mg, 0.592 mmol) and hydrazine hydrate (0.074 mL, 1.184 mmol, ~50% in H_2O) in 6 mL ethanol was stirred for one hour at room temperature. The solid was filtered and dried under high vacuum to provide 118.5 mg (82.3%) of **CDE-492** as a white solid. ^1H NMR ($\text{DMSO-}d_6$, 400 MHz) δ 9.99 (bs, 1H), 8.97 (t, $J=6$ Hz, 1H), 7.2 (q, $J=8.2$ Hz, 1H), 6.92 (t, $J=9$ Hz, 1H), 4.47 (bs, 2H), 4.34 (d, $J=5.5$ Hz, 2H), 2.14 (s, 3H). ^{13}C NMR ($\text{DMSO-}d_6$, 100 MHz) δ 160.04, 159.66 (dd, $J=8.58$ Hz, $J=244.1$ Hz), 159.57 (dd, $J=8.59$ Hz, $J=246.0$ Hz), 158.39, 131.14 (dd, $J=6.7$ Hz, $J=9.5$ Hz), 120.60 (dd, $J=3.81$ Hz, $J=18.11$ Hz), 113.58 (t, $J=19.1$ Hz), 111.20 (dd, $J=3.8$ Hz, $J=21.9$ Hz), 31.57, 14.25 (d, $J=2.9$ Hz); HRMS, DART calcd. for $\text{C}_{10}\text{H}_{11}\text{F}_2\text{N}_3\text{O}_2$ $[\text{M}+\text{H}^+]$ 244.08976, found: 244.08900.

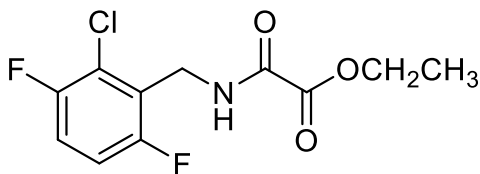


Ethyl 2-oxo-2-((2,3,4-trifluorobenzyl)amino)acetate (KMU-1-12): The procedure for the synthesis of **KMU-1-1** was followed, substituting 4-(difluoromethoxy)-benzylamine for 2,3,4-

trifluorobenzylamine which gave 420.6 mg (88.1%) of **KMU-1-12** as an off-white solid. ^1H NMR (CDCl_3 , 400 MHz) δ 7.43 (bs, 1H), 7.10 (m, 1H), 6.93 (ddt, $J=6.9$ Hz, $J=6.9$ Hz, $J=6.9$ Hz, 1H), 4.54 (d, $J=6.4$ Hz, 2H), 4.34 (q, $J=6.8$ Hz, 2H), 1.38 (t, $J=6.9$ Hz, 3H).

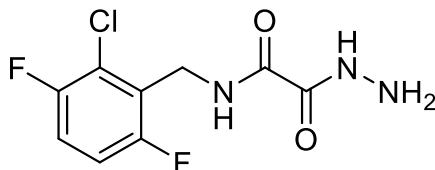


2-hydrazinyl-2-oxo-N-(2,3,4-trifluorobenzyl)acetamide (CDE-493): A solution of **KMU-1-12** (139.9 mg, 0.538 mmol) and hydrazine hydrate (0.067 mL, 1.071 mmol, ~50% in H_2O) in 6 mL ethanol was stirred for one hour at room temperature with manual breakup of the solid required. The sturdy solid was filtered and dried under high vacuum to provide 104.2 mg (78.8%) of **CDE-493** as an off-white stiff solid. ^1H NMR ($\text{DMSO}-d_6$, 400 MHz) δ 10.04 (bs, 1H), 9.28 (t, $J=6$ Hz, 1H), 7.24 (m, 1H), 7.11 (m, 1H), 4.51 (bs, 2H), 4.32 (d, $J=6$ Hz, 2H). ^{13}C NMR ($\text{DMSO}-d_6$, 100 MHz) δ 160.53, 158.25, 149.90 (ddd, $J=2.8$ Hz, $J=9.5$ Hz, $J=245.0$ Hz), 148.96 (ddd, $J=2.8$ Hz, $J=10.5$ Hz, $J=247.0$ Hz), 139.33 (dt, $J=15.3$ Hz, $J=246.9$ Hz), 124.37 (m), 124.10 (dd, $J=2.8$ Hz, $J=12.4$ Hz), 112.90 (dd, $J=2.8$ Hz, $J=16.2$ Hz), 36.06; HRMS, DART calcd. for $\text{C}_9\text{H}_8\text{F}_3\text{N}_3\text{O}_2$ [$\text{M}+\text{H}^+$] 248.06468, found: 248.06300.

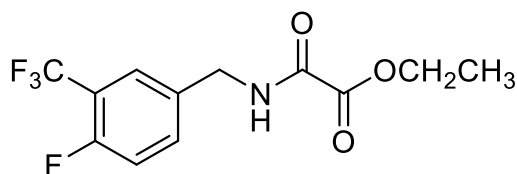


Ethyl 2-((2-chloro-3,6-difluorobenzyl)amino)-2-oxoacetate (KMU-1-8): The procedure for the synthesis of **KMU-1-1** was followed, substituting 4-(difluoromethoxy)-benzylamine for 2-chloro-3,6-difluorobenzylamine which gave 401.2 mg (79.1%) of **KMU-1-8** as an off-white

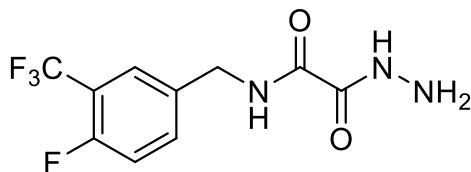
solid. ^1H NMR (CDCl_3 , 400 MHz) δ 7.35 (bs, 1H), 7.12 (m, 1H), 7.01 (m, 1H), 4.71 (dd, $J=1.4$ Hz, $J=6.0$ Hz, 2H), 4.33 (q, $J=7.4$ Hz, 2H), 1.37 (t, $J=6.9$ Hz, 3H).



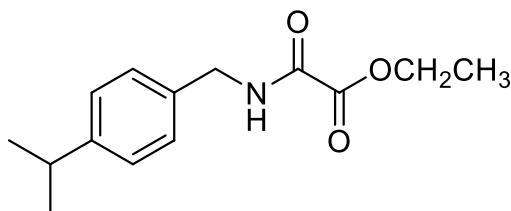
N-(2-chloro-3,6-difluorobenzyl)-2-hydrazinyl-2-oxoacetamide (CDE-494): A solution of **KMU-1-8** (148.8 mg, 0.536 mmol) and hydrazine hydrate (0.067 mL, 1.072 mmol, ~50% in H_2O) in 4 mL ethanol was stirred for one hour at room temperature. The solid was filtered and dried under high vacuum to provide 87.2 mg (61.8%) of **CDE-494** as a white, granular solid. ^1H NMR ($\text{DMSO}-d_6$, 400 MHz) δ 10.01 (bs, 1H), 9.03 (bs, 1H), 7.39 (m, 1H), 7.24 (m, 1H) 4.49 (bs, 2H), 4.42 (d, $J=5.5$ Hz, 2H). ^{13}C NMR ($\text{DMSO}-d_6$, 100 MHz) δ 160.19, 158.26, 157.64 (d, $J=244.1$ Hz), 154.45 (d, $J=240.1$ Hz), 125.52 (d, $J=19.1$ Hz), 121.91 (dd, $J=19.1$ Hz, $J=5.7$ Hz), 116.90 (dd, $J=23.8$ Hz, $J=9.5$ Hz), 115.62 (dd, $J=25.7$ Hz, $J=8.6$ Hz), 35.16; HRMS, DART calcd. for $\text{C}_9\text{H}_8\text{ClF}_2\text{N}_3\text{O}_2$ [$\text{M}+\text{H}^+$] 264.03514, found: 264.03601.



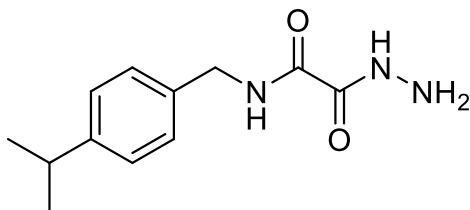
Ethyl 2-((4-fluoro-3-(trifluoromethyl)benzyl)amino)-2-oxoacetate (KMU-1-11): The procedure for the synthesis of **KMU-1-1** was followed, substituting 4-(difluoromethoxy)-benzylamine for 4-fluoro-3-(trifluoromethyl)benzylamine which gave 462.5 mg (86.2%) of **KMU-1-11** as a yellow solid. ^1H NMR (CDCl_3 , 400 MHz) δ 7.51 (m, 3H), 7.18 (t, $J=9.6$ Hz, 1H), 4.53 (d, $J=6.4$ Hz, 2H), 4.36 (q, $J=7.3$ Hz, 2H), 1.39 (t, $J=6.9$ Hz, 3H).



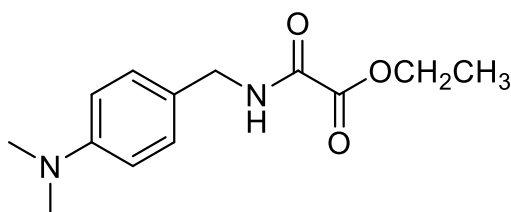
N-(4-fluoro-3-(trifluoromethyl)benzyl)-2-hydrazinyl-2-oxoacetamide (CDE-495): A solution of **KMU-1-11** (140.8 mg, 0.480 mmol) and hydrazine hydrate (0.060 mL, 0.961 mmol, ~50% in H₂O) in 5.1 mL ethanol was stirred for one hour at room temperature. The solid was filtered and dried under high vacuum to provide 90.6 mg (67.6%) of **CDE-495** as a white solid. ¹H NMR (DMSO-*d*₆, 400 MHz) δ 10.04 (bs, 1H), 9.36 (t, *J*=6 Hz, 1H), 7.64 (d, *J*=6.9 Hz, 1H), 7.59 (m, 1H), 7.42 (t, *J*=10.5 Hz, 1H), 4.50 (bs, 2H), 4.32 (d, *J*=6 Hz, 2H). ¹³C NMR (DMSO-*d*₆, 100 MHz) δ 160.53, 158.35, 158.32 (d, *J*=252.7 Hz), 136.54 (d, *J*=2.9 Hz), 134.81 (d, *J*=8.6 Hz), 126.69 (d, *J*=3.8 Hz), 122.52 (q, *J*=269.8 Hz), 117.61 (d, *J*=21.0 Hz), 116.70 (dd, *J*=31.5 Hz, *J*=12.4 Hz), 41.72; HRMS, DART calcd. for C₁₀H₉F₄N₃O₂ [M+H⁺] 280.07090, found: 280.06799.



Ethyl 2-((4-isopropylbenzyl)amino)-2-oxoacetate (KMU-1-17): The procedure for the synthesis of **KMU-1-1** was followed, substituting 4-(difluoromethoxy)-benzylamine for 4-isopropylbenzylamine which gave 367.0 mg (80.7%) of **KMU-1-17** as a pale white solid. ¹H NMR (CDCl₃, 400 MHz) δ 7.32 (bs, 1H), 7.22 (m, 4H), 4.47 (d, *J*=6 Hz, 2H), 4.34 (q, *J*=7.3 Hz, 2H), 2.9 (sep, *J*=6.9 Hz, 1H), 1.38 (t, *J*=7.3 Hz, 3H), 1.23 (d, *J*=6.9 Hz, 6H).

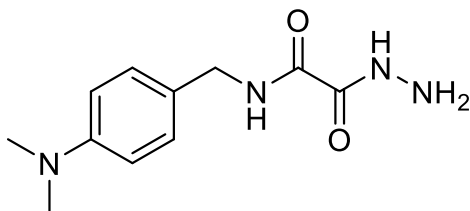


2-hydrazinyl-N-(4-isopropylbenzyl)-2-oxoacetamide (CDE-496): A solution of **KMU-1-17** (160.1 mg, 0.642 mmol) and hydrazine hydrate (0.080 mL, 1.284 mmol, ~50% in H₂O) in 6 mL ethanol was stirred for one hour at room temperature with manual breakup of the solid required. The solid was filtered and dried under high vacuum to provide 118.4 mg (78.7%) of **CDE-496** as a hard white solid. ¹H NMR (DMSO-*d*₆, 400 MHz) δ 10.00 (bs, 1H), 9.17 (t, *J*=6.4 Hz, 1H), 7.14 (s, 4H), 4.50 (bs, 2H), 4.24 (d, *J*=6.4 Hz, 2H), 2.81 (sep, *J*=7.3 Hz, 1H), 1.13 (d, *J*=6.9 Hz, 6H). ¹³C NMR (DMSO-*d*₆, 100 MHz) δ 160.26, 158.64, 147.58, 136.77, 127.94, 126.68, 42.44, 33.65, 24.46; HRMS, DART calcd. for C₁₂H₁₇N₃O₂ [M+H⁺] 236.13991, found: 236.13901.

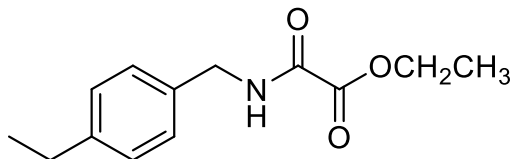


Ethyl 2-((4-(dimethylamino)benzyl)amino)-2-oxoacetate (KMU-1-19): To a solution of 4-(dimethylamino)benzylamine (0.270 mL, 1.83 mmol) and triethylamine (0.509 mL, 3.66 mmol) in 2.05 mL of CH₂Cl₂ stirred in an ice bath, ethylchlorooxoacetate (0.21 mL, 1.92 mmol) was added dropwise. The reaction was allowed to stir for one hour. The reaction mixture was then diluted with 30 mL ethyl acetate and washed with 2 × 25 mL of 0.2N HCl, followed by 2 × 25 mL sat. aqueous NaHCO₃. The organic phase was then dried with anhydrous MgSO₄, filtered and concentrated to provide 766.0 mg (quantitative yield) of **KMU-1-19** as an impure solid. ¹H

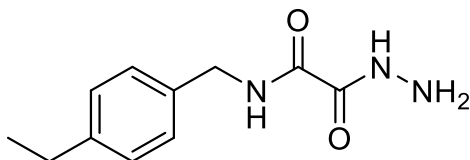
NMR (CDCl₃, 400 MHz) δ 7.29 (m, 1H), 6.66 (m, 4H), 4.4 (d, $J=5.5$ Hz, 2H), 4.24 (q, $J=7.3$ Hz, 2H), 2.94 (s, 6H), 1.36 (m, 3H).



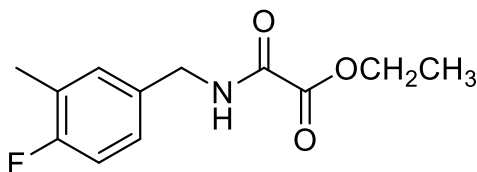
N-(4-(dimethylamino)benzyl)-2-hydrazinyl-2-oxoacetamide (CDE-497): A solution of **KMU-1-19** (199.2 mg, 0.796 mmol) and hydrazine hydrate (0.099 mL, 1.592 mmol, ~50% in H₂O) in 4 mL ethanol was stirred for one hour at room temperature. The solid was filtered and dried under high vacuum to provide 37.5 mg (20.0%) of **CDE-497** as a white solid. ¹H NMR (DMSO-*d*₆, 400 MHz) δ 9.97 (bs, 1H), 9.02 (t, $J=6$ Hz, 1H), 7.05 (d, $J=8.3$ Hz, 2H), 6.62 (d, $J=8.7$ Hz, 2H), 4.46 (bs, 2H), 4.15 (d, $J=6.4$ Hz, 2H), 2.81 (s, 6H). ¹³C NMR (DMSO-*d*₆, 100 MHz) δ 160.01, 158.74, 150.16, 128.98, 126.89, 112.80, 42.23, 40.79; HRMS, DART calcd. for C₁₁H₁₆N₄O₂ [M+H⁺] 237.13514, found: 237.13499.



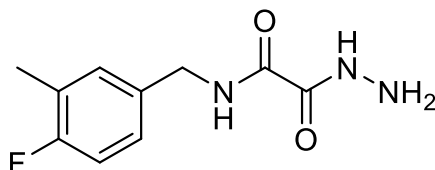
Ethyl 2-((4-ethylbenzyl)amino)-2-oxoacetate (KMU-1-22): The procedure for the synthesis of **KMU-1-1** was followed, substituting 4-(difluoromethoxy)-benzylamine for 4-ethylbenzylamine which gave 341.0 mg (79.4%) of **KMU-1-22** as a yellow oil. ¹H NMR (CDCl₃, 400 MHz) δ 7.32 (bs, 1H), 7.19 (q, $J=8.2$ Hz, 4H), 4.47 (d, $J=6$ Hz, 2H), 4.34 (q, $J=6.9$ Hz, 2H), 2.63 (q, $J=7.8$ Hz, 2H), 1.38 (t, $J=6.9$ Hz, 3H), 1.22 (t, $J=7.3$ Hz, 3H).



N-(4-ethylbenzyl)-2-hydrazinyl-2-oxoacetamide (CDE-498): A solution of **KMU-1-22** (138.5 mg, 0.589 mmol) and hydrazine hydrate (0.073 mL, 1.178 mmol, ~50% in H₂O) in 4 mL ethanol was stirred for one hour at room temperature. The solid was filtered and dried under high vacuum to provide 100.8 mg (76.9%) of **CDE-498** as an off-white solid. ¹H NMR (DMSO-*d*₆, 400 MHz) δ 9.99 (s, 1H), 9.16 (t, *J*=6.4 Hz, 1H), 7.12 (q, *J*=5 Hz, 4H), 4.49 (bs, 2H), 4.24 (d, *J*=6.4 Hz, 2H), 2.52 (q, *J*=7.3 Hz, 2H), 1.12 (t, *J*=7.3 Hz, 3H). ¹³C NMR (DMSO-*d*₆, 100 MHz) δ 160.26, 158.64, 142.92, 136.62, 128.17, 127.94, 42.44, 28.34, 16.27; HRMS, DART calcd. for C₁₁H₁₅N₃O₂ [M+H⁺] 222.12425, found: 222.12199.

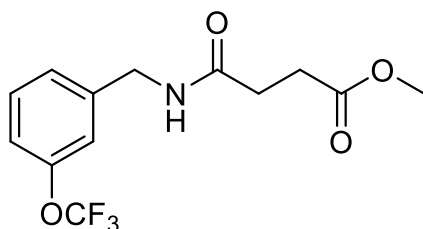


Ethyl 2-((4-fluoro-3-methylbenzyl)amino)-2-oxoacetate (KMU-1-23): The procedure for the synthesis of **KMU-1-1** was followed, substituting 4-(difluoromethoxy)-benzylamine for 4-fluoro-3-methylbenzylamine which gave 341.0 mg (79.4%) of **KMU-1-22** as a yellow oil. ¹H NMR (CDCl₃, 400 MHz) δ 7.34 (bs, 1H), 7.08 (m, 2H), 6.96 (t, *J*=9.2 Hz, 1H), 4.43 (d, *J*=6 Hz, 2H), 4.34 (q, *J*=7.4 Hz, 2H), 2.25 (d, *J*=1.8 Hz, 3H), 1.38 (t, *J*=7.3 Hz, 3H).

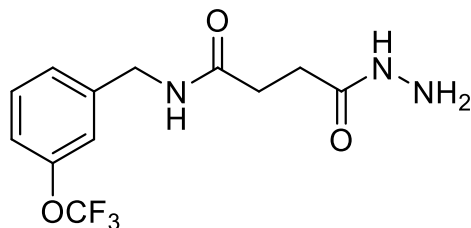


N-(4-fluoro-3-methylbenzyl)-2-hydrazinyl-2-oxoacetamide (CDE-499): A solution of **KMU-1-23** (186.9 mg, 0.782 mmol) and hydrazine hydrate (0.097 mL, 1.563 mmol, ~50% in H₂O) in 4

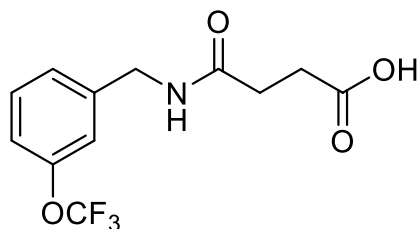
mL ethanol was stirred for one hour at room temperature. The solid was filtered and dried under high vacuum to provide 149.6 mg (85.5%) of **CDE-499** as a white solid. ^1H NMR (DMSO- d_6 , 400 MHz) δ 10.00 (s, 1H), 9.2 (t, $J=6$ Hz, 1H), 7.05 (m, 3H), 4.49 (bs, 2H), 4.22 (d, $J=6.4$ Hz, 2H), 2.16 (s, 3H). ^{13}C NMR (DMSO- d_6 , 100 MHz) δ 160.29, 160.20 (d, $J=240.3$ Hz), 158.57, 135.22 (d, $J=3.8$ Hz), 131.13 (d, $J=5.7$ Hz), 127.18 (d, $J=7.6$ Hz), 124.30 (d, $J=17.2$ Hz), 115.17 (d, $J=22.9$ Hz), 42.01, 14.67 (d, $J=2.9$ Hz); HRMS, DART calcd. for $\text{C}_{10}\text{H}_{12}\text{FN}_3\text{O}_2$ [M+H $^+$] 226.09918, found: 226.09900.



Methyl 4-oxo-4-((3-(trifluoromethoxy)benzyl)amino)butanoate (CDE-501): To a solution of 3-(trifluoromethoxy)benzylamine (1.03 mL, 3.66 mmol) and pyridine (1.16 mL, 3.84 mmol) in CH_2Cl_2 (20 mL) stirred in an ice bath, methyl-4-chloro-4-oxobutyrate (1.16 mL, 7.32 mmol) was added dropwise. The reaction was allowed to react overnight, warming to room temperature. The solution was then diluted with ethyl acetate and washed with 2×25 mL 0.2N HCl and 2×25 mL NaHCO_3 . The organic phase was dried with anhydrous MgSO_4 , filtered and dried under vacuum to yield 1.7634 g (80.1%) of a viscous off-white material. ^1H NMR (CDCl_3 , 400 MHz) δ 7.34 (t, $J=8.7$ Hz, 1H), 7.19 (d, $J=7.4$ Hz, 1H), 7.11 (bs, 2H), 6.10 (bs, 1H), 4.45 (d, $J=6$ Hz, 2H), 3.68 (m, 3H), 2.61 (tt, $J=6.9$ Hz, $J=73.8$ Hz, 4H). ^{13}C NMR (CDCl_3 , 100 MHz) δ 173.57, 171.63, 149.53, 140.86, 130.07, 125.95, 120.50 (q, $J=255.5$ Hz), 120.09, 119.83, 51.92, 43.00, 30.99, 19.33; HRMS, DART calcd. for $\text{C}_{13}\text{H}_{14}\text{F}_3\text{NO}_4$ [M+H $^+$] 306.09532, found: 306.09799.

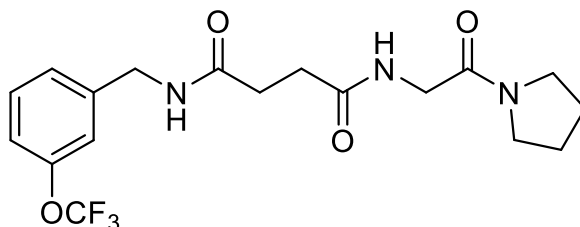


4-hydrazinyl-4-oxo-N-(3-(trifluoromethoxy)benzyl)butanamide (CDE-502): A solution of **CDE-501** (121.0 mg, 0.397 mmol) and hydrazine hydrate (0.247 mL, 3.970 mmol, ~50% in H₂O) in ethanol 3.90 mL was allowed to stir overnight. 2 drops of RO H₂O was added and product formation was verified via TLC (30:70 EtOAc:Hexanes). The solution was rotovapped and dried under vacuum, giving yield to 92.4 mg (73.4%) of a white solid, **CDE-502**. ¹H NMR (DMSO-*d*₆, 400 MHz) δ 8.93 (bs, 1H), 8.41 (t, J=5.5 Hz, 1H), 7.41 (m, 1H), 7.20 (m, 3H), 4.26 (d, J=6 Hz, 2H), 4.09 (bs, 2H), 2.37 (m, 2H), 2.24 (m, 2H). ¹³C NMR (DMSO-*d*₆, 100 MHz) δ 172.00, 171.37, 148.96, 143.19, 130.41, 126.67, 120.77 (q, J=254.6 Hz), 119.99, 119.64, 41.97, 31.16, 29.37; HRMS, DART calcd. for C₁₂H₁₄F₃N₃O₃ [M+H⁺] 306.10655, found: 306.10001.

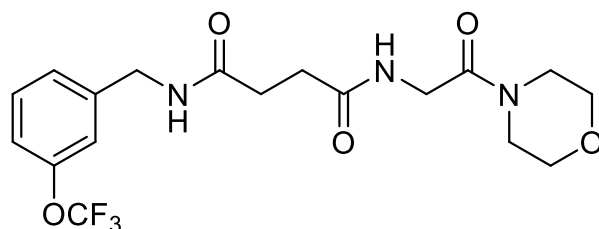


4-oxo-4-((3-(trifluoromethoxy)benzyl)amino)butanoic acid (CDE-503): A solution of **CDE-501** (494.1 mg, 1.62 mmol) in 4 mL EtOH, 5 M NaOH (1.296 mL, 6.48 mmol) was added and allowed to stir overnight. The reaction solution was diluted with 30 mL EtOAc, and washed with 2 × 25 mL 0.2 N HCl and 2 × 25 mL brine. The organic layer was dried with MgSO₄, filtered and the solvent was evaporated to yield 386.5 mg (82.0%) of **CDE-503** as a brittle white solid.

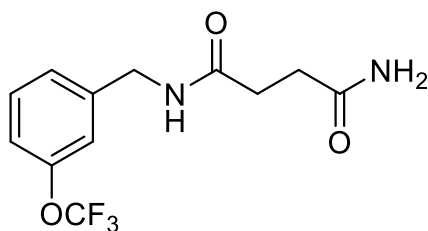
^1H NMR (DMSO- d_6 , 400 MHz) δ 12.05 (bs, 1h), 8.41 (t, $J=5.9$ Hz, 1H), 7.41 (m, 1H), 7.24 (d, $J=7.8$ Hz, 1H), 7.19 (bs, 2H), 4.27 (d, $J=6$ Hz, 2H), 2.38 (m, 4H). ^{13}C NMR (DMSO- d_6 , 100 MHz) δ 174.38, 171.79, 148.98, 143.21, 130.67, 126.63, 120.47 (q, $J=254.6$ Hz), 119.96, 119.63, 41.97, 30.45, 29.57; HRMS, DART calcd. for $\text{C}_{12}\text{H}_{12}\text{F}_3\text{NO}_4$ [$\text{M}+\text{H}^+$] 292.07966, found: 292.08099.



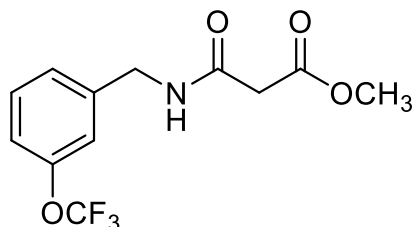
N1-(2-oxo-2-(pyrrolidin-1-yl)ethyl)-N4-(3-(trifluoromethoxy)benzyl)succinamide (CDE-504): To a solution of **CDE-503** (95.6 mg, 0.328 mmol) in 6 mL CH_2Cl_2 , 2-amino-1-pyrrolidin-1-yl-ethanone hydrochloride (108.4 mg, 0.658 mmol), DMF (0.6 mL), HOBt \cdot H_2O (61.6 mg, 0.455 mmol), N-methylmorpholine (0.072 mL, 0.655 mmol) were added with stirring in an ice bath, followed by the addition of EDC \cdot HCl (75.7 mg, 0.395 mmol). The reaction mixture was allowed to stir overnight. The stir bar was then removed and solvent was evaporated. A solution of 4:1 EtOAc:hexanes (30 mL) was then added and transferred to a separatory funnel, leaving a yellow oil behind. The organic layer was washed with 2×25 mL 0.1N NaOH and 2×25 mL brine, dried with anhydrous MgSO_4 , filtered, and concentrated to give 67.9 mg (51.8%) of **CDE-504** as a white, granular solid. ^1H NMR (DMSO- d_6 , 400 MHz) δ 8.39 (t, $J=6$ Hz, 1H), 7.94 (t, $J=5.5$ Hz, 1H), 7.39 (t, $J=8.7$ Hz, 1H), 7.24 (d, $J=7.8$ Hz, 1H), 7.19 (s, 2H), 4.26 (d, $J=6$ Hz, 2H), 3.79 (d, $J=5.5$ Hz, 2H), 3.34 (m, 2H), 3.25 (m, 2H), 2.38 (m, 4H), 1.78 (m, 4H). ^{13}C NMR (DMSO- d_6 , 100 MHz) δ 172.11, 171.99, 148.99, 143.22, 130.67, 126.66, 120.52 (q, $J=254.6$ Hz), 119.99, 119.61, 46.04, 45.44, 41.97, 41.79, 31.27, 31.02, 26.14, 24.22; HRMS, DART calcd. for $\text{C}_{18}\text{H}_{22}\text{F}_3\text{N}_3\text{O}_4$ [$\text{M}+\text{H}^+$] 402.16408, found: 402.16199.



N1-(2-morpholino-2-oxoethyl)-N4-(3-(trifluoromethoxy)benzyl)succinamide (CDE-505): To a solution of **CDE-503** (100.9 mg, 0.347 mmol) in 6.1 mL CH₂Cl₂, 2-amino-1-morpholino-1-ethanone hydrochloride (125.1 mg, 0.693 mmol), DMF (0.5 mL), HOBt · H₂O (58.8 mg, 0.435 mmol), N-methylmorpholine (0.076 mL, 0.691 mmol) were added with stirring in an ice bath, followed by the addition of EDC · HCl (80.5 mg, 0.420 mmol). The reaction mixture was allowed to stir overnight. The stir bar was then removed and solvent was evaporated. A solution of 4:1 EtOAc:hexanes (30mL) was then added and transferred to a separatory funnel, leaving a yellow oil behind. The organic layer was washed with 2 × 25 mL 0.1N NaOH and 2 × 25 mL brine, dried with anhydrous MgSO₄, filtered, and concentrated to give 62.2 mg (43.2%) of **CDE-505** as a white solid. ¹H NMR (DMSO-*d*₆, 400 MHz) δ 8.39 (t, J=5.5 Hz, 1H), 7.95 (t, J=5 Hz, 1H), 7.41 (t, J=7.8 Hz, 1H), 7.24 (d, J=7.3 Hz, 1H), 7.19 (bs, 2H), 4.26 (d, J=6 Hz, 2H), 3.89 (d, J=5.5 Hz, 2H), 3.51 (bs, 4H), 3.81 (bs, 4H). ¹³C NMR (DMSO-*d*₆, 100 MHz) δ 172.09, 172.00, 167.78, 148.98, 143.22, 130.68, 126.66, 120.75 (q, J=254.6), 119.99, 119.63, 66.51 (d, J=6.7 Hz), 45.08, 40.65, 40.45, 31.21, 31.03; HRMS, DART calcd. for C₁₈H₂₂F₃N₃O₅ [M+H⁺] 418.15898, found: 418.15302.

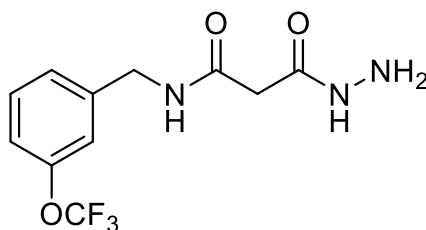


N1-(3-(trifluoromethoxy)benzyl)succinamide (CDE-506): 124.2 mg (0.407 mmol) of **CDE-501** was added to a reaction vial with a stir bar followed by the dropwise addition of ammonia in methanol (4.0 mL, 181.0 mmol, 7 N). The solution was allowed to react overnight. TLC in 50:50 EtOAc:hexanes the next day showed that not all starting material had been consumed and therefore more ammonia in methanol (2 mL, 90.0 mmol, 7 N) as well as ethanol (0.5 mL) was added and allowed to react overnight. The solution was then rotovapped and the resulting solid was triturated with chloroform to produce 44.0 mg (37.3%) of **CDE-506** as a white, granular solid. ¹H NMR (DMSO-*d*₆, 400 MHz) δ 8.38 (t, J=5.9 Hz, 1H), 7.39 (m, 1H), 7.24 (d, J=7.8 Hz, 2H), 7.19 (s, 2H), 6.69 (s, 1H), 4.26 (d, J=6 Hz, 2H), 2.31 (m, 4H). ¹³C NMR (DMSO-*d*₆, 100 MHz) δ 173.91, 172.25, 148.97, 143.27, 130.68, 126.64, 121.20 (q, J=254.6 Hz), 119.97, 119.62, 41.95, 31.04, 30.84; HRMS, DART calcd. for C₁₂H₁₃F₃N₂O₃ [M+H⁺] 291.09565, found: 291.09601.

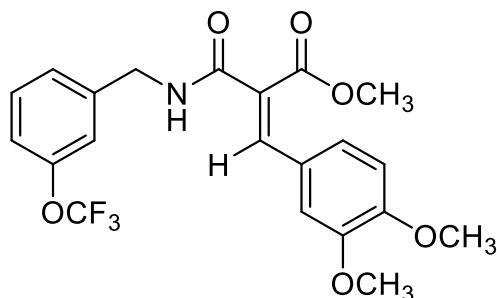


Methyl 3-oxo-3-((3-(trifluoromethoxy)benzyl)amino)propanoate (CDE-509): To a solution of 3-(trifluoromethoxy)benzylamine (1.03 mL, 7.22 mmol), pyridine (1.16 mL, 14.44 mmol), and CH₂Cl₂ (20.5 mL) stirring in an ice bath, methyl malonyl chloride (0.812 mL, 7.58 mmol) was added dropwise. The solution noticeably changed vibrant colors, from neon orange to yellow, back to orange, upon the addition of methyl malonyl chloride. The reaction was allowed to stir, warming to room temp, for 24 hours. The CH₂Cl₂ was then evaporated and the remainder diluted with ethyl acetate (40 mL). The solution was then washed with 3 × 25 mL 0.2N HCl and 3 × 25 mL sat. NaHCO₃, dried with anhydrous MgSO₄, filtered and concentrated to provide 1.8915 g

(90.0%) of crude material. Column chromatography was performed using a gradient of 20%, 40%, and 75% EtOAc:hexanes as the eluent to give 602.8 mg (28.7%) of **CDE-509** as a powdery white solid. TLC confirmed **CDE-509** to have an r.f. of 0.4 in 75% EtOAc:hexanes. ^1H NMR (CDCl_3 , 400 MHz) δ 7.53 (bs, 1H), 7.35 (t, $J=7.8$ Hz, 1H), 7.21 (d, $J=7.8$ Hz, 1H), 7.13 (s, 1H), 7.11 (bs, 1H), 4.5 (d, $J=6$ Hz, 2H), 3.74 (s, 3H), 3.38 (s, 2H). ^{13}C NMR ($\text{DMSO}-d_6$, 100 MHz) δ 170.09, 165.03, 149.57, 140.41, 130.16, 125.98, 120.80 (q, $J=255.5$ Hz), 120.17, 119.95, 52.61 (m), 42.98, 40.79; HRMS, DART calcd. for $\text{C}_{12}\text{H}_{12}\text{F}_3\text{NO}_4$ $[\text{M}+\text{H}^+]$ 292.07966, found: 292.07599.

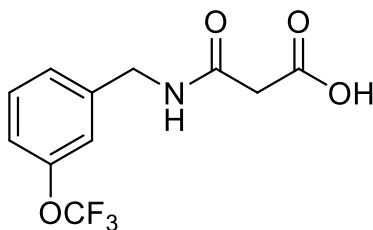


3-hydrazinyl-3-oxo-N-(3-(trifluoromethoxy)benzyl)propanamide (CDE-511): 73.5 mg (0.253 mmol) of **CDE-509** was dissolved in EtOH (2 mL) and hydrazine hydrate (0.128 mL, 1.012 mmol, ~50% in H_2O) was added. The reaction was monitored by TLC and after 8 hours all starting material had been consumed. The solution was rotovapped and concentrated to give 67.9 mg (92.3%) of **CDE-511** as a white solid. ^1H NMR ($\text{DMSO}-d_6$, 400 MHz) δ 9.09 (bs, 1H), 8.52 (t, $J=6$ Hz, 1H), 7.42 (t, $J=7.8$ Hz, 1H), 7.29 (d, $J=7.3$ Hz, 1H), 7.23 (s, 1H), 7.21 (d, $J=7.8$ Hz, 1H), 4.29 (d, $J=5.9$ Hz, 2H), 4.22 (bs, 2H), 3.00 (s, 2H). ^{13}C NMR ($\text{DMSO}-d_6$, 100 MHz) δ 167.35, 166.71, 148.99, 142.84, 130.70, 126.69, 120.40 (q, $J=254.6$ Hz), 120.06, 119.71, 42.28, 42.13; HRMS, DART calcd. for $\text{C}_{11}\text{H}_{12}\text{F}_3\text{N}_3\text{O}_3$ $[\text{M}+\text{H}^+]$ 292.09089, found: 292.09201.

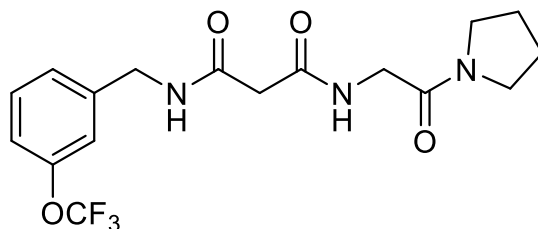


(Z)-methyl 3-(3,4-dimethoxyphenyl)-2-((3-(trifluoromethoxy)benzyl)carbamoyl)acrylate

(CDE-512): CDE-509 (74.4 mg, 0.256 mmol), veratraldehyde (214.8 mg, 1.28 mmol), and piperidine (0.006 mL, 0.064 mmol) were placed in a microwave tube and subjected to irradiation for 7.5 minutes at 100 °C at 250W. The solution was then diluted with EtOAc (30 mL) and washed with 2 × 25 mL 0.1N HCl. The solution was then concentrated to give 265.2 mg (100%) of crude material. The material was then subjected to column chromatography with 40% EtOAc:hexanes as the eluent. 133.9 mg (100%) of crude material was recovered from the column and triturated with hexanes to yield 30.8 mg (27.4%) of **CDE-512** as a white crystalline solid. ¹H NMR (CDCl₃, 400 MHz) δ 7.71 (s, 1H), 7.32 (t, J=7.8 Hz, 1H), 7.2 (d, J=7.8 Hz, 1H), 7.14 (bs, 3H), 7.11 (d, J=2.3 Hz, 1H), 6.8 (d, J=9.2 Hz, 1H), 6.19 (t, J=5.9 Hz, 1H), 4.59 (d, J=6.4 Hz, 2H), 3.90 (s, 3H), 3.84 (s, 3H), 3.79 (s, 3H). ¹³C NMR (CDCl₃, 100 MHz) δ 166.84, 165.66, 151.45, 149.57, 148.99, 143.00, 140.07, 130.11, 126.04, 125.76, 125.58, 124.60, 120.27 (q, J=256.5 Hz), 120.25, 119.99, 112.30, 110.96, 55.98, 55.87, 52.59, 43.08; HRMS, DART calcd. for C₂₁H₂₀F₃NO₆ [M+H⁺] 440.13209, found: 440.12799.

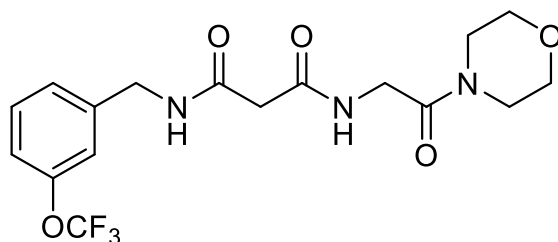


3-oxo-3-((3-(trifluoromethoxy)benzyl)amino)propanoic acid (CDE-521): CDE-509 (332.0 mg, 1.140 mmol) was dissolved in EtOH (6.90 mL) with stirring in an ice bath. 5M NaOH (0.92 mL, 4.562 mmol) was added dropwise and the reaction was allowed to proceed overnight at room temperature. The solution was diluted with chilled 30 mL CH₂Cl₂ and washed 2 × 25 mL chilled 0.2N HCl and 2 × 25 mL chilled brine. The organic layers were then dried with anhydrous MgSO₄, filtered and concentrated via rotovap at low heat to give 197.0 mg (62.3%) of **CDE-521** as an off-white brittle solid. ¹H NMR (DMSO-*d*₆, 400 MHz) δ 8.61 (t, J=6 Hz, 1H), 7.42 (t, J=7.8 Hz, 1H), 7.27 (m, 2H), 7.23 (d, J=6 Hz, 1H), 4.31 (d, J=6 Hz, 2H), 3.18 (s, 2H). ¹³C NMR (DMSO-*d*₆, 100 MHz) δ 170.04, 166.53, 149.02, 142.76, 130.70, 126.67, 120.61 (q, J=254 Hz), 120.00, 119.77, 43.19, 42.06; HRMS, DART calcd. for C₁₁H₁₀F₃NO₄ [M+H⁺] 278.06401, found: 278.06601.



N1-(2-oxo-2-(pyrrolidin-1-yl)ethyl)-N3-(3-(trifluoromethoxy)benzyl)malonamide (CDE-522): To a solution of **CDE-521** (68.5 mg, 0.250 mmol) in 7.5 mL CH₂Cl₂, 2-amino-1-pyrrolidin-1-yl-ethanone hydrochloride (85.7 mg, 0.500 mmol), DMF (0.51 mL), HOBT · H₂O (49.0 mg, 0.300 mmol), N-methylmorpholine (0.0550 mL, 0.500 mmol) were added with stirring in an ice bath, followed by the addition of EDC · HCl (53.8 mg, 0.300 mmol). The reaction mixture was allowed to stir overnight. The stir bar was then removed and solvent was evaporated. A solution of 4:1 EtOAc:hexanes (30 mL) was then added and transferred to a separatory funnel, leaving a yellow viscous material behind. The organic layer was washed with 2 × 25 mL 0.2N NaOH and 2 × 25 mL brine, dried with anhydrous MgSO₄, filtered, and

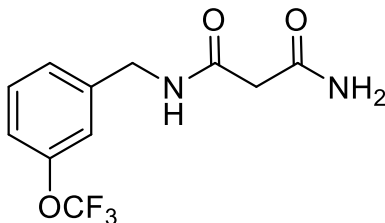
concentrated. The off-white crystalline solid was then triturated with hexanes to give 31.9 mg (33.2%) of **CDE-522** as a white powdery solid. ^1H NMR (CDCl_3 , 400 MHz) δ 7.86 (bs, 1H), 7.34 (t, $J=7.8$ Hz, 1H), 7.23 (d, $J=7.8$ Hz, 1H), 7.10 (m, 3H), 4.47 (d, $J=6$ Hz, 2H), 3.97 (d, $J=4.1$ Hz, 2H), 3.49 (t, $J=6.9$ Hz, 2H), 3.37 (t, $J=6.4$ Hz, 2H), 3.31 (s, 2H), 1.93 (m, 4H). ^{13}C NMR (CDCl_3 , 100 MHz) δ 168.12, 166.46, 165.93, 149.50, 140.67, 130.06, 126.03, 120.51 (q, $J=255$ Hz), 120.21, 119.76, 46.19, 45.60, 26.00, 24.20; HRMS, DART calcd. for $\text{C}_{17}\text{H}_{20}\text{F}_3\text{N}_3\text{O}_4$ $[\text{M}+\text{H}^+]$ 388.14842, found: 388.14401.



N1-(2-morpholino-2-oxoethyl)-N3-(3-(trifluoromethoxy)benzyl)malonamide (CDE-523):

To a solution of **CDE-521** (82.0 mg, 0.300 mmol) in 6.0 mL CH_2Cl_2 , 2-amino-1-morpholino-1-ethanone hydrochloride (109.2 mg, 0.600 mmol), DMF (0.50 mL), HOBt \cdot H_2O (55.3 mg, 0.360 mmol), N-methylmorpholine (0.0660 mL, 0.600 mmol) were added with stirring in an ice bath, followed by the addition of EDC \cdot HCl (68.7 mg, 0.360 mmol). The reaction mixture was allowed to stir overnight. The stir bar was then removed and solvent was evaporated. A solution of 4:1 EtOAc:hexanes (30 mL) was then added and transferred to a separatory funnel, leaving a yellow viscous material behind. The organic layer was washed with 2×25 mL 0.2N NaOH and 2×25 mL brine, dried with anhydrous MgSO_4 , filtered, and concentrated. The white solid was then triturated with hexanes to give 57.1 mg (47.2%) of **CDE-523** as a white solid. ^1H NMR (CDCl_3 , 400 MHz) δ 7.63 (bs, 1H), 7.34 (t, $J=7.4$ Hz, 1H), 7.21 (d, $J=7.8$ Hz, 1H), 7.17 (bs, 1H), 7.12 (bs, 1H), 7.10 (bs, 1H), 4.49 (d, $J=6$ Hz, 2H), 4.05 (d, $J=4.1$ Hz, 2H), 3.67 (m, 6H), 3.39 (t,

J=5.0 Hz, 2H), 3.30 (s, 2H) ^{13}C NMR (CDCl_3 , 100 MHz) δ 167.94, 166.51, 166.24, 149.50, 140.47, 130.09, 126.03, 120.50 (q, J=255 Hz), 120.17, 119.82, 66.67, 66.35, 44.93, 42.93, 42.75, 42.42, 41.30; HRMS, DART calcd. for $\text{C}_{17}\text{H}_{20}\text{F}_3\text{N}_3\text{O}_5$ [M+H⁺] 404.14332, found: 404.14099.



N1-(3-(trifluoromethoxy)benzyl)malonamide (CDE-524): CDE-509 (71.4 mg, 0.245 mmol) was dissolved in ammonia in methanol (28.1 mL, 1273 mmol, 7 N) in an ice bath and stirred for 3.5 hours. The vial was then moved to cold storage for an additional 9 hours at which time the solution was tested via TLC using 1:1 EtOAc:hexanes to verify all starting material had been consumed and no side products were produced. The solvent was evaporated and the solution concentrated to give 52.0 mg (77.6%) of **CDE-524** as a green-tinted tacky solid. ^1H NMR (CDCl_3 , 400 MHz) δ 7.63 (bs, 1H), 7.32 (t, J=8.2 Hz, 1H), 7.25 (s, 1H), 7.17 (d, J=7.8 Hz, 1H), 7.11 (s, 1H), 7.00 (bs, 1H), 5.80 (bs, 1H), 4.43 (d, J=17 Hz, 2H), 3.24 (s, 2H). ^{13}C NMR (CDCl_3 , 100 MHz) δ 169.88, 167.27, 149.55, 140.26, 130.16, 125.89, 120.51 (q, J=255 Hz), 120.11, 119.96, 43.03, 42.68; HRMS, DART calcd. for $\text{C}_{11}\text{H}_{11}\text{F}_3\text{N}_2\text{O}_3$ [M+H⁺] 277.08000, found: 277.07901.